THE UNIVERSITY OF ALBERTA

THE THERMODYNAMICS OF ICING SPRAYS

by

© HEATHER EVA AULD

A THESIS

SUBMITTED TO THE FACULTY OF GRADUATE STUDIES AND RESEARCH

IN PARTIAL FULFILMENT OF THE REQUIREMENTS FOR THE DEGREE

OF MASTER OF SCIENCE

IN

METEOROLOGY

DEPARTMENT OF GEOGRAPHY

EDMONTON, ALBERTA

FALL, 1980

Dedication

To my parents

In appreciation of so many things

ABSTRACT

The design of anti-icing protective devices for aircraft requires that they be checked for operational effectiveness in a testing facility. For one such facility, the icing wind tunnel, the method used to simulate the icing cloud is to inject a continuous spray of water droplets into a cold airstream. These simulated conditions were investigated in this thesis using a one-dimensional numerical model.

The purpose of this study was to formulate a model of general applicability that determined the spray and air thermodynamics and dynamics in any test facility. The governing equations were programmed in FORTRAN IV language for solution on a digital computer. The temperatures and velocities of the spray droplets and the air, averaged over a cross-sectional area perpendicular to the tunnel axis, were calculated. Two models -- a single droplet model and a droplet ensemble model -- were developed. The equations of the two models treat a frictionless, adiabatic flow in which the total entropy of the system is conserved. The equations of the single droplet model apply to situations where the spray has a negligible influence on the air flow. The ensemble model is applicable for cases where the contributions of the spray (consisting of N identical droplets per unit volume) to the moist air have to be considered.

A limited parametric study was performed to determine the effects of moist air properties at the tunnel plenum (beginning of contraction) and of initial water spray conditions on the state of the flow at the

working section of the NRC* high speed tunnel. The results indicate that the downstream spray properties (at the tunnel working section section))are essentially independent of the initial spray liquid content, injection temperature, and relative velocity (with respect to the air). The spray temperature is sensitive to the tunnel relative humidity and tends to approach the wet-bulb temperature of the air. Smaller droplets (10 microns) approach the wet-bulb temperature and the velocity of the air sooner than larger droplets (100 microns). When plenum conditions are adjusted to give air speeds at the working section of 30 m/s and 60 m/s, a spray of 25 micron droplets reaches the air temperature and velocity before arriving at the working section of the NRC tunnel. The spray remains substantially out of equilibrium with the air when the final air speed is near 130 m/s.

---

* National Research Council

ACKNOWLEDGEMENTS

I wish to express my gratitude to Dr. Edward Lozowski for finding time in a busy schedule to supervise my study and for having assisted in the preparation of this thesis. I also would like to thank Dr. R. B. Charlton and Dr. E. M. Gates for serving on my examining committee.

My sincerest appreciation goes to my dear friend and colleague, Mr. Doug Phillips, for his keen interest in my study, for his original suggestions, and for his valuable assistance with so many other aspects of this thesis.

I am deeply grateful to Ms. Laura Smith for her aid in typing the equations. Her many offers of help will certainly be remembered. I also thank my colleague, Mr. Randy Rudolph, for sharing his typewriter.

I would like to thank my conscientious typist, Ms. Debi Stephens, for her speedy and expert work.

Finally, I thank the Natural Sciences and Engineering Research Council for providing support in the form of a fellowship during my first two years of graduate study. The final draft of this thesis was written while on educational leave from the Atmospheric Environment Service, Environment Canada.

TABLE OF CONTENTS

LIST OF TABLES

LIST OF FIGURES

CHAPTER 1

INTRODUCTION

1.1 An Introduction to the Icing Problem

The formation of ice on aircraft surfaces occurs during flight through clouds of supercooled water droplets. Because these supercooled water droplets are in a state of metastable equilibrium, the disturbance created by a moving aircraft causes the impinging droplets to form ice on its nucleating surfaces.

The ice accretion on aircraft surfaces always results in a degradation of its performance and reduces its operational safety. The result of ice accretion may be malfunctions of essential instruments, a reduction of aerodynamic lift, an increase in drag, an increase in weight, and an impairment of manoeuverability. Icing of propellers and rotor blades may also lead to a considerable reduction of forward thrust. In the case of turbine-type aircraft, ice released from the inlet duct of the engine may damage fan and compressor blades and may cause compressor flame-out (Vath, 1978). Because of these effects, aircraft are routinely equipped with protective systems for either removing accumulated ice or for continuously maintaining the exposed surfaces of the aircraft free from ice. These protective devices must be tested for operational effectiveness under conditions that closely simulate or duplicate the natural atmospheric icing conditions. A good simulation thus requires that the primary variables defining icing conditions be established and controlled in the testing facility during the testing process. The purpose of this thesis is to analyze the conditions that are simulated in an icing wind tunnel.

Here at the University of Alberta, the Department of Mechanical Engineering has developed an icing wind tunnel to simulate natural atmospheric icing conditions. An icing wind tunnel has also been developed at the National Research Council (NRC) in Ottawa. Chapter 4 of this thesis describes the numerically sinulated icing conditions that result from a high speed air flow in the NRC tunnel. For a general description of the NRC tunnel, the reader is referred to Section 1.3. The next section presents a survey of natural icing conditions.

1.2 Natural Icing Conditions

In general, ice formation results from a complex interaction of aerodynamic and meteorological factors. The aerodynamic factors include the aircraft speed, skin temperature, and the size and shape of the icing surfaces. The meteorological factors include pressure, air humidity, liquid water content and cloud ice, cloud droplet size and size distribution, and cloud temperature. The degree or severity of icing may be described as light, moderate, or severe (Vath, 1978), but these are relative terms. The difficulty with them, from a meteorologist's point of view, is that they are usually aircraft specific. Thus, light icing for a Boeing 747 may be severe for a helicopter, for example.

There are three types of atmospheric ice formation, namely clear ice, rime ice, and mixed or intermediate ice. Clear ice generally forms with air temperatures in the range of 0°C to -10°C, where freezing is very slow. Here, larger supercooled droplets that collect on the aircraft surfaces partly freeze on impact, while the rest of the droplet runs back prior to freezing. The resulting ice formation is dense and adheres tightly

to the surface. The liquid water content of clouds producing clear icing is a large one ($\sim 1 g/m^3$) because of the larger droplet size. Rime ice, on the other hand, forms at low temperatures (as low as -40°C) and usually forms on aircraft surfaces from flight in clouds with low liquid water contents. This ice form accumulates on the leading edges of aircraft wings and other surfaces and results from small droplets freezing on the airframe individually with little or no spreading. The physical appearance of rime ice, often described as friable, is milky white (due to the presence of air pockets) and its structure is porous and the surface rough. Rime ice tends to build forward from exposed surfaces and accumulates less quickly than clear ice due to the generally lower liquid water contents of clouds producing this type of icing. Mixed or intermediate ice, as its name suggests, has some characteristics of both types of ice.

The three types of ice formation described above may be associated with the following major types of icing environments: stratiform or layer clouds, cumuliform clouds, and freezing rain or other low level icing. The stratiform clouds, with low to moderate liquid water contents, have a long horizontal extent and are associated with continuous icing. The cumuliform clouds, with moderate to high liquid water contents, have a vertical extent comparable to the horizontal extent, and are associated with intermittent icing. The freezing rain and freezing drizzle situations (i.e. moist layer(s) above the surface characterized by temperatures near freezing) are associated with severe continuous clear icing.

The icing intensities associated with the different cloud types are described in Table 1.1. It is emphasized that various types

TABLE 1.1

ICING POTENTIAL ASSOCIATED WITH THE VARIOUS CLOUD TYPES (AFTER MASON, 1957)

Type of Cloud*	Intensity of Icing	Probability that ice will accumulate	Water content (g/m^3) of cloud
Tcu, Cb, Ns	May be severe	High	0.2 - 4.0
Sc, Ac Ac with As	Light-Moderate	$\approx$50%	0.1 - 0.5
As	Light-Moderate	Low	0.1 - 0.3
St	Light	Low	0.1 - 0.5

* Tcu Towering Cumulus
Cb Cumulonimbus
Ns Nimbostratus
Sc Stratocumulus
Ac Altocumulus
As Altostratus
St Stratus
Cu Cumulus

and degrees of icing are possible in convective type clouds with clear icing often observed. In the case of Sc type clouds formed over the sea and Sc formed by the spreading out of Cu, moderate to severe mixed or clear icing may occur.

The fact that ice formation differs from aircraft type to aircraft type results in a rather subjective classification of the different degrees of icing. Despite this subjectivity, standard icing conditions have been formulated for the purpose of testing aircraft performance. The icing criteria are based on flights made with specially instrumented aircraft through weather conditions that have resulted in icing. Since these standard icing conditions are defined in terms of the typical speeds, rates of climb and performance of a particular aviation era, the standard icing conditions can become outdated as aircraft performance improves. It is emphasized that the specifications used in testing an aircraft's ability to withstand icing pertain specifically to icing on external aerodynamic surfaces and not to engine performance icing conditions.

1.3 The NRC High Speed Icing Tunnel

A vertical cross-section of the NRC high speed icing wind tunnel is shown in Figure 1.1. The portion of the tunnel where icing conditions are simulated consists of 1) a rapidly converging bell-mouth contraction followed by 2) a more gentle linear contraction and 3) a working section of constant dimensions. (See upper left hand portion of Figure 1.1.) An analytic expression for the variation of the cross-sectional area along the tunnel axis appears in Appendix H. This cross-section is square throughout the tunnel.

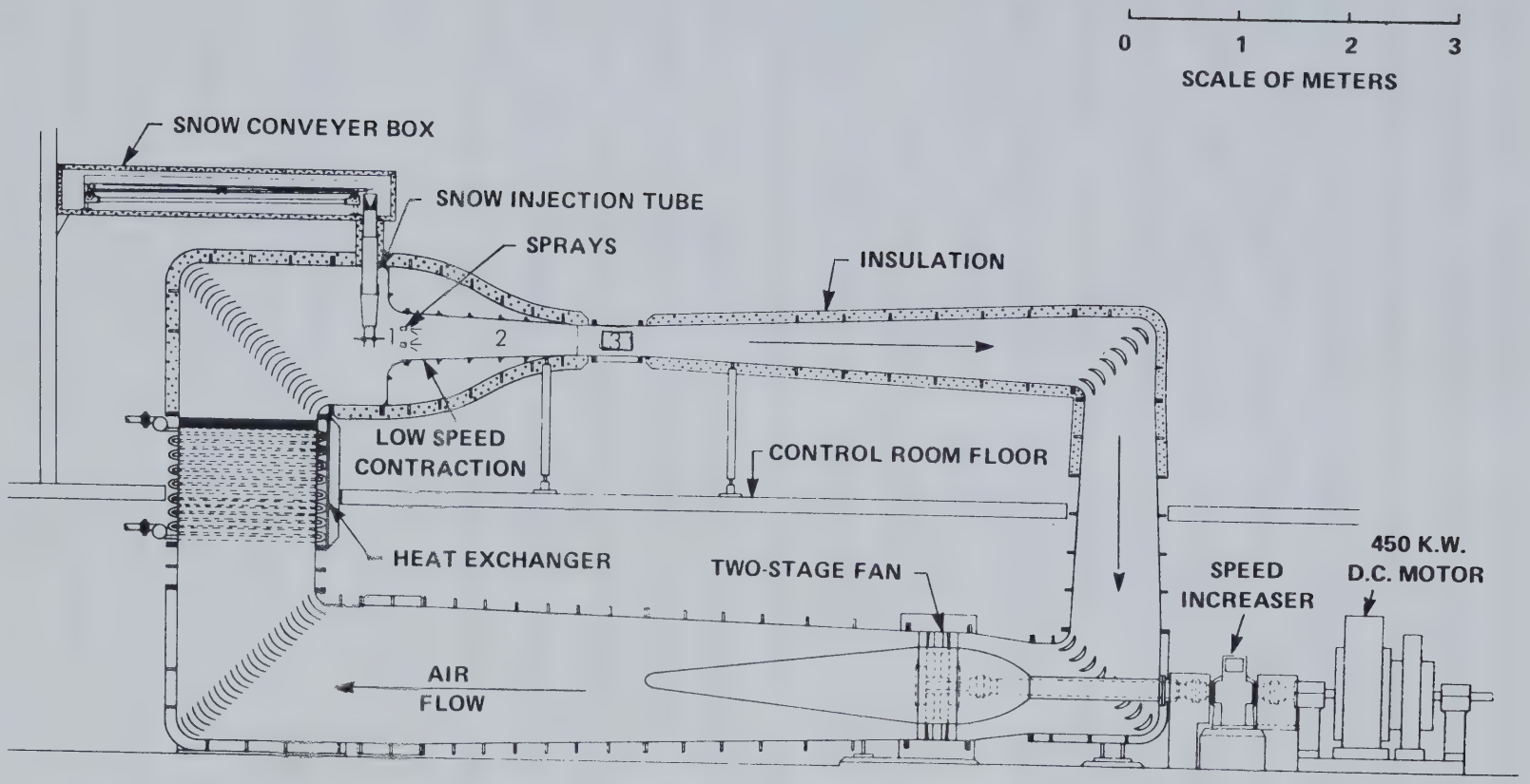

FIGURE 1.1 : Vertical cross-section of the NRC high speed icing wind tunnel. The low speed contraction is the tunnel configuration of interest. The portion of the tunnel where icing conditions are simulated consists of 1) a rapidly converging bell-mouth followed by 2) a more gentle linear contraction and 3) a working section of constant dimensions.
(after Lozowski et al., 1979)

Briefly, the method used at NRC to produce an icing cloud is to inject a continuous spray of water droplets into a cold airstream. The droplet spray is produced by four pneumatic atomizing nozzles located 0.20 m downstream from the plenum (beginning of contraction). The water supply to the spray nozzles is usually at room temperature while the compressed air supply needed to produce the spray is heated to 30°or 40°C. Since both the water flow rate and the atomizing air pressure are roughly controllable, the liquid water content of the spray and median volume radius of the droplets are roughly known. On the other hand, the spray temperature, injection velocity, and the precise location of the droplet formation are unknown.

For most experimental and modeling situations, it is assumed that the droplet attains the temperature and velocity of the airflow by the time that the spray reaches the working or test section of the tunnel. This assumption is generally valid for slower tunnel speeds. For the higher tunnel speeds (greater than 90 m/s in the working section) and large accelerations, there may be insufficient time for the spray to reach thermal and dynamical equilibrium with the airstream, especially if the airstream itself is cooling by adiabatic expansion and accelerating.

1.4 Purpose of the Study

As mentioned earlier, the purpose of this study is to analyze the conditions that are simulated in an icing tunnel. The problem to be considered is to determine the temperature and velocity of the spray and moist air in the working section of the tunnel. For many testing situations, measurements of these properties are either not feasible or are

subject to significant error. It is also desirable to determine the initial conditions that are required in order to produce given icing conditions at the working section. The approach used in this study is to numerically determine these flow properties from a model. The numerical models that were developed to simulate these conditions are discussed in Chapters 2 and 3. Results describing the numerical simulation in the NRC high speed tunnel are discussed in Chapter 4.

CHAPTER 2

THE SINGLE DROPLET MODEL

2.1 Outline

The liquid water contents found in a cloud environment are simulated in an icing tunnel by injecting water droplets, known as a spray, from atomizing nozzles into a moist air flow. The problem of modeling the thermodynamics of the injected spray is to describe the two phase flow of a water suspension in air. The medium considered consists of moist air and fine liquid droplets that are, for practical purposes, accelerated by the viscous drag of the accelerating air. The droplets are assumed to be spherical, rigid, and incompressible and their specific volume is assumed negligible compared to the gas phase. In addition, the effects of droplet coagulation are neglected.

A description of the dynamics of the two phase flow uses the fundamental conservation laws for mass, energy, and momentum. The balance equations are written for air and for the droplet, respectively. These equations account for mass, momentum, and energy exchanges between the air and the droplets.

The two sets of equations, with their inherent assumptions, constitute the models of the present study. The equations are solved numerically. One set of equations describes the properties of the system where a single droplet is injected into the moist air flow. The second set describes the properties of the system where an ensemble of N identical droplets per unit volume is injected into the air flow. In the discussions that follow, the first model is referred to as the "single droplet model" while the second model is referred to as the "ensemble model".

Both models treat the flow in the tunnel as a one-dimensional steady flow.

The two-dimensional nature of the tunnel flow is ignored in both models. Instead, general one-dimensional equations are obtained from the use of spatial averaging techniques. The variables used in this study are considered to be averaged over a cross-sectional area that is normal to the tunnel axis and are functions only of the distance x along the tunnel axis from the plenum (beginning of contraction). A number of other averaging techniques may be employed in engineering applications when treating one-dimensional averaged variables. These include (Solbrig and Hughes, 1978, p. 310) volume averaging of variables, spatial averaging of the equations of motion, and statistical methods of averaging.

The advantage of using one-dimensional averaged variables is that the resulting flow equations are simplified and become very general. When using averaged variables, however, it is important that the information obtained from solving the flow equations be carefully interpreted.

Appendix 1 contains a summary of the variables used in the text. Variables are also defined in the text as they are introduced. Variables describing properties of the dry air, vapor, and the droplets are denoted by the subscripts d, v, and c (condensed phase), respectively, while variables without subscripts refer to properties of the moist air (dry air plus water vapor).

2.2 Dry Air Flow in a Wind Tunnel

Many wind tunnels are designed with an objective of obtaining an air flow in the working section that has a uniform, rectilinear velocity profile. For a properly designed tunnel, the velocity over a

cross-section of the working section (outside of a thin boundary layer), described as a flow area, may be treated as constant. In the contraction section, the component of velocity perpendicular to the tunnel axis is treated as negligible if the curvature of the locus of the center points of the flow areas is small and if the tunnel boundary layer is thin. In such cases, the flow area is approximately the cross-sectional area and the averaged velocity is approximately the axial velocity.

The following analysis of one-dimensional flow in a wind tunnel describes a positive distance x as the distance along the tunnel axis from an origin at the plenum. The portion of the tunnel considered is the contraction and working sections.

The relationship between pressure and velocity at different points of a fluid field can, in general, be obtained from an analysis of the dynamics of a particle of the fluid. The relation is obtained from the simultaneous solution of the energy, continuity, and momentum equations, and from the equation of state.

The equation of state adopted for the dry air is the Perfect Gas Law, written as

$$\frac{P}{\rho} = R_d T \qquad (2.2.1)$$

where

P is pressure,

ρ is density,

T is temperature, and

R_d is the specific gas constant for dry air.

Corrections for moist air, to avoid a variable gas constant, are made later.

The momentum equations describing the motion are the Navier-Stokes equations. Their complete solution is very complex unless a number of simplifying assumptions can be applied to the flow. The equations of motion reduce to the compressible Bernoulli equation if it is assumed that the flow is:

1) steady (does not vary with time locally) and,

2) inviscid (viscous or frictional forces are negligible).

If the flow is treated as a one-dimensional flow, the analysis is simplified further. The Bernoulli equation for a one-dimensional flow can be written as:

$$\frac{U_2^2}{2} - \frac{U_1^2}{2} + \int_{P_1}^{P_2} \frac{dP}{\rho} + g(z_2 - z_1) = 0 \qquad (2.2.2)$$

where U refers to velocity, z is the vertical distance from the tunnel axis, and g is the acceleration of gravity. The subscripts 1 and 2 refer to values of the variables at the positions x_1 and x_2, respectively. For the tunnel with velocities greater than 10 m/s and vertical scale of a few meters, scale analysis shows that the gravitational term in the above expression is neglected relative to the other terms.

When the walls of the tunnel are assumed to be insulated and all other heat sources or sinks are negligible, the steady-state thermodynamic equation describes an isentropic flow of a perfect gas. The adiabatic expansion and compression of the air is described by the relation,

$$\frac{P_1}{\rho_1^{\gamma}} = \frac{P_2}{\rho_2^{\gamma}} \qquad (2.2.3)$$

and $\gamma = c_p/c_v = 1.4$ for dry air.

Finally, if mass is conserved, the steady-state mass continuity equation is easily integrated for the one-dimensional flow. The equation describing mass continuity of the dry air flux is,

$$\rho_2 U_2 A_2 = \rho_1 U_1 A_1 \qquad (2.2.4)$$

where A is the cross-sectional area.

For adiabatic flow where mass is conserved, the momentum and energy equations can be combined to give an expression for the velocity. The relations describing the state of the moving air are as follows:

1. Bernoulli equation (2.2.2),
2. Dry adiabatic expansion (2.2.3),
3. Mass continuity equation (2.2.4).

If (2.2.3) is substituted into (2.2.2), neglecting the gravity term, the resulting equation may be integrated to give,

$$\frac{U_2^2}{2} + \frac{\gamma}{\gamma-1}\frac{P_2}{\rho_2} = \frac{U_1^2}{2} + \frac{\gamma}{\gamma-1}\frac{P_1}{\rho_1} \qquad (2.2.5)$$

Equations 2.2.3 and 2.2.4 are combined to give the expression,

$$\frac{P_2}{\rho_2} = \frac{P_1}{\rho_2}\left[\frac{U_1 A_1}{U_2 A_2}\right]^{\gamma-1} \qquad (2.2.6)$$

If (2.2.6) is substituted into (2.2.5), an equation is obtained that relates the fluid velocity and the cross-sectional area at a point along the tunnel axis to known variables at another point. The equation that results,

$$\frac{U_2^2}{2} + \frac{P_1}{\rho_1}\left[\frac{U_1 A_1}{U_2 A_2}\right]^{\gamma-1}\left(\frac{\gamma}{\gamma-1}\right) = \frac{U_1^2}{2} + \frac{P_1}{\rho_1}\left(\frac{\gamma}{\gamma-1}\right) \qquad (2.2.7)$$

can then be solved numerically to yield the velocity, U_2, for any cross-sectional area in the x-direction.

Using the one-dimensional velocity, the density is determined from the continuity equation using the relation,

$$\rho_2 = \frac{\rho_1 U_1 A_1}{\rho_2 U_2}$$

The remaining equations, the adiabatic expansion relation and the Perfect Gas Law, can be applied to obtain the pressure and the temperature, respectively. In addition, the dimensionless Mach number, M, can be calculated using the above quantities. The Mach number for adiabatic flow of the dry air (treated as a perfect gas) is given by,

$$M = \frac{U}{\sqrt{\gamma R_d T}} \qquad (2.2.8)$$

Equations 2.2.2, 2.2.3, and 2.2.4 can also be rewritten in terms of the Mach number. The derivations are given in Appendix 2.

A numerical solution to (2.2.7) can be obtained using the observation that $U_2^2/2$ is small compared to the second term on the left hand side for velocities of interest. If (2.2.7) is rewritten as

$$\frac{\gamma}{\gamma-1}\frac{P_1}{\rho_1}\left(\frac{U_1 A_1}{A_2}\right)^{\gamma-1} U_2^{1-\gamma} = \frac{U_1^2}{2} - \frac{U_2^2}{2} + \frac{P_1}{\rho_1}\left(\frac{\gamma}{\gamma-1}\right) \qquad (2.2.9)$$

it is found that the resulting expression is particularly suited to yield a numerical solution for the velocity by an iterative technique. A first guess of the unknown velocity, U_2, on the right hand side is the velocity obtained under the assumption of incompressible flow. The expression for the first guess velocity, denoted $U_2^{(0)}$, is

$$U_2^{(0)} = \frac{U_1 A_1}{A_2}$$

An improved estimate of the root is written as,

$$U^{(n+1)} = \left\{ \left[(U_1^2 - U_2^2)^{(n)} + \frac{2P_1}{\rho_1} \frac{\gamma}{\gamma-1} \right] \Big/ \left(\frac{\gamma}{\gamma-1} \frac{2P_1}{\rho_1} \left[\frac{U_1 A_1}{A_2} \right]^{(\gamma-1)} \right) \right\}^{\frac{1}{1-\gamma}} \tag{2.2.10}$$

where $U^{(n+1)}$ refers to the $(n+1)$th estimate of the one-dimensional velocity, U_2.

2.3 Moist Air Flow

When modeling the moist air flow in an icing tunnel, the equations of motion must account for the presence of water vapor. In practice, the water vapor contribution to the moist air density is relatively small and, depending on the accuracy required, some calculations may neglect this component. In the following discussion, the vapor contribution to the moist air density is treated as constant since it is assumed that evaporation or condensation does not occur. As a result, the inclusion of water vapor will alter only the definitions of the variables characterizing the flow.

A number of variables are defined in the meteorological literature to describe the water vapor content of moist air. One such moisture variable, the mixing ratio, r, is defined as the ratio of the density of water vapor to the density of dry air; that is, $r = \rho_v/\rho_d$. Using the Perfect Gas Law for each component, this ratio is also written as, $r = \frac{\varepsilon e}{P_d}$, where $\varepsilon = R_d/R_v = 0.62198$ and R_v is the specific gas constant for water vapor. P_d and e are the dry air and water vapor partial pressures, respectively.

A humidity variable, virtual temperature, incorporates a moisture correction into the temperature. The virtual temperature is defined as the temperature at which dry air would have the same density as a sample of moist air, assuming both have the same pressure. Its use allows the equation of state for dry air to be written for the moist air without resorting to a humidity-dependent gas constant. The general formula for the virtual temperature, T' , is

$$T' = T\left(1 + \frac{0.6098r}{r+1}\right) \qquad (2.3.1)$$

Using the definition of virtual temperature, the equation of state for moist air is,

$$P = P_d + e = \rho R_d T'$$

where $\rho = \rho_d + \rho_v$. When reference is made to the moist air temperature (which for a dry air and vapor system in thermal equilibrium is also the temperature of the dry air and of the vapor), it will be denoted as T.

As mentioned, only the definitions of the parameters and variables used in the equations of motion for the dry air flow will require modification when water vapor is a part of the air flow. For example, the equation of state for moist air specifies that the pressure and density refer to their moist air values and that the temperature used is the virtual temperature. The Bernoulli equation is likewise unchanged in form when the moist air variables are used and is given by (2.2.2). Since it is assumed that the mixing ratio remains constant for this flow, the steady-state continuity equation for the moist air implies continuity of the dry air flux, Equation 2.2.4. In addition, Poisson's equation (2.2.3) for an adiabatic expansion of an ideal gas from the state P_1, ρ_1

to the state P_2, ρ_2 applies for the moist air flow if the exponent, $\gamma = c_p/c_v$, is determined as a function of the mixing ratio of the moist air. Expressions for the heat capacities of moist air, c_p and c_v, are derived in Iribarne and Godson (1973, p. 70) and can be written as,

$$c_p = c_{pd}\left[1 + \frac{r}{r+1}\left(\frac{c_{pv}}{c_{pd}} - 1\right)\right], \quad c_v = c_{vd}\left[1 + \frac{r}{r+1}\left(\frac{c_{vv}}{c_{vd}} - 1\right)\right] \tag{2.3.2}$$

Here, c_{pv} and c_{pd} are the specific heat capacities at constant pressure for water vapor and dry air, respectively and c_{vv} and c_{vd} refer to specific heat capacities at constant volume for water vapor and dry air, respectively. It is seen from (2.3.2) that the specific heat, capacities remain constant for a constant mixing ratio, as does the exponent γ.

Since the equations describing the moist air flow are identical in form to those describing the dry air flow when the mixing ratio is constant, the velocity equation derived in the previous section applies to the moist air flow. The one-dimensional velocity is then solved using the iteration equation (2.2.10). Following the analysis of the previous section, the moist air density is determined from the continuity equation. The moist air pressure, virtual temperature, and the thermodynamic temperature, T, are then found using the adiabatic expansion equation, the Perfect Gas Law, and the definition of virtual temperature, respectively.

2.4 Droplet Motion

The motion of a single droplet in air is governed by Newton's Second Law of Motion, where the forces considered are the gravity force and the drag of the air on the droplet. The gravity force may be neglected

relative to the drag force for the droplet sizes (of the order of 10-100 microns) and accelerations considered in this study.

The problem of determining the droplet motion in a viscous medium is a complicated one since the drag force is a function of the droplet size, relative velocity of the droplet with respect to the air, the viscosity of the air, and of time. Three of these variables can be combined to form a ratio, the Reynolds number, that characterizes the viscous flow. The ratio is given by,

$$Re = \frac{2r_c\rho}{\mu} | U - U_c | = \frac{2r_c | U - U_c |}{\nu} \qquad (2.4.1)$$

where the variable, r_c, refers to the radius of the droplet, μ is the dynamic viscosity of the air, and $\nu = \mu/\rho$ is the kinematic viscosity of the air. It is assumed that the droplet remains spherical.

A related problem, the determination of the steady-state drag on a sphere, has been the subject of a considerable number of theoretical and empirical studies. A convenient summary of these investigations, as well as a discussion of a numerical study to extend the applicable range of the past investigations, is presented in a paper by LeClair et al.(1970).

For droplets approximated as rigid spheres, the numerical study of LeClair et al.(1970) is able to theoretically predict accurate values of the drag over a Reynolds number range from 0.01 to 400. Their theoretically determined solutions agree excellently with experimental drag determinations by Beard and Pruppacher (1969). The study by Beard and Pruppacher measures the drag on water drops falling at terminal velocity in air for the Reynolds number range 0.2 to 200 and extrapolates these results to a Reynolds number of 400, numerically. The agreement of the theoretical and numerical results is given as evidence that the droplets

can be modeled as rigid spheres for Reynolds numbers in this range. The empirical drag relation described by Beard and Pruppacher's results is,

$$\frac{F}{F_{Stokes}} = 1 + \alpha Re^{\beta} \qquad (2.4.2)$$

where

$\alpha = 0.102$, $\beta = 0.995$ for $0.01 \leq Re \leq 1.5$,

$\alpha = 0.115$, $\beta = 0.802$ for $1.5 \leq Re < 20$,

$\alpha = 0.189$, $\beta = 0.632$ for $20 \leq Re < 400$

Here, F is the steady-state drag on the spherical droplet and F_{Stokes} is the Stokes drag given by,

$$F_{Stokes} = 6\pi\mu r_c (U - U_c)$$

The steady-state drag given by Equation 2.4.2 is not adequate for many situations where the droplet undergoes large accelerations. For example, preliminary calculations for droplet motion through the contraction section of the high speed icing tunnel at NRC in Ottawa (to be discussed later) indicate that additional terms should be included in the equations of motion to account for the time dependency. An analytical solution to the non-steady state problem, for Reynolds numbers less than 0.01, has been obtained by Pearcy and Hill (1956). The drag force predicted by solving the Navier-Stokes equations is

$$F_{drag} = 2\pi\rho r_c^3 \left\{ \frac{3\nu(U-U_c)}{r_c^2} + \frac{1}{3}\frac{d}{dt}(U-U_c) \right.$$

$$\left. + \frac{3}{r_c}\sqrt{\frac{\nu}{\pi}} \int_{-\infty}^{t} \frac{d(U-U_c)}{d\tau} \frac{d\tau}{\sqrt{t-\tau}} \right\} \qquad (2.4.3)$$

The first term is the steady-state viscous force arising from uniform motion (i.e. Stokes drag). The second force term is associated with the momentum transferred to the surrounding medium by changes in the velocity of the droplet. The third term, known as the history term, represents resistance due to the expenditure of energy needed to set the fluid in motion. The integrand of the history term indicates that the effect of past accelerations decreases with time (proportional to $t^{-1/2}$)

The Stokes drag term in Equation 2.4.3 is corrected using the steady-state results of Beard and Pruppacher (Equation 2.4.2). This leads to

$$F_{drag} = m_c \frac{dU_c}{dt} = 2\pi\rho r_c^3 \left\{ \frac{3\nu(U-U_c)}{r_c^2} (1+\alpha Re^{\beta}) + \frac{1}{3}\frac{d}{dt}(U-U_c) \right.$$

$$\left. + \frac{3}{r_c}\sqrt{\frac{\nu}{\pi}} \int_{-\infty}^{t} \frac{d(U-U_c)}{d\tau} \frac{d\tau}{\sqrt{t-\tau}} \right\} \qquad (2.4.4)$$

In most of the literature on droplet motion, the steady-state drag forces are used to predict the motion of water droplets in a viscous medium. Justification for neglecting the history term is generally not offered. An empirical study by Sartor and Abbott (1975) concludes that steady-state drag forces can be used to describe the motion of an accelerating droplet that is falling in a straight path and is characterized by a Reynolds number less than 5. An investigation by P. I. Joe (1975) highly recommends that the history term be included in the drag formulation of accelerating droplets when the motion is along curvilinear paths and for large Reynolds numbers. The study shows that, for intermediate or large Reynolds numbers ($Re \geq 10$), errors of at least 25 percent can result when calculating droplet velocities.

If the full history term is included, determination of the time dependent motion is not trivial, since the solution of the differential equation for the droplet motion (Equation 2.4.4) first requires integration of the history term. In order to simplify the calculations, the history term is omitted from the drag equation that is solved numerically in both models. It is realized that the error due to its neglect may be significant.

Figures 2.1a and 2.1b show the results of a numerical experiment performed to estimate the relative importance of the history term for high speed flow in the NRC tunnel. The experiment calculates the ratio of the force given by the history term to the steady-state horizontal drag force as a function of the distance, x, the droplet travel time, and the droplet initial conditions. A first approximation to the history term is obtained using velocities that were given by the equations of motion from which the history term had been omitted. The droplet radius used in this experiment is 10 microns. The air speed at the sprayers is 51 m/s and the corresponding air temperature is 1°C.

The Figures indicate that the relative importance of the history term is strongly dependent upon the droplet initial conditions (that is, the droplet history). It is seen that the drag force is always of greater magnitude than the history term. For the case where the droplet injection velocity is zero (and the initial relative velocities are large), the Figure indicates that the history term is relatively unimportant for a large fraction of the travel time. It is noted, however, that the history term is of significance for droplet motion near the sprayers. For the case where the droplet is injected with the air speed, the initial drag forces are extremely small and the history term

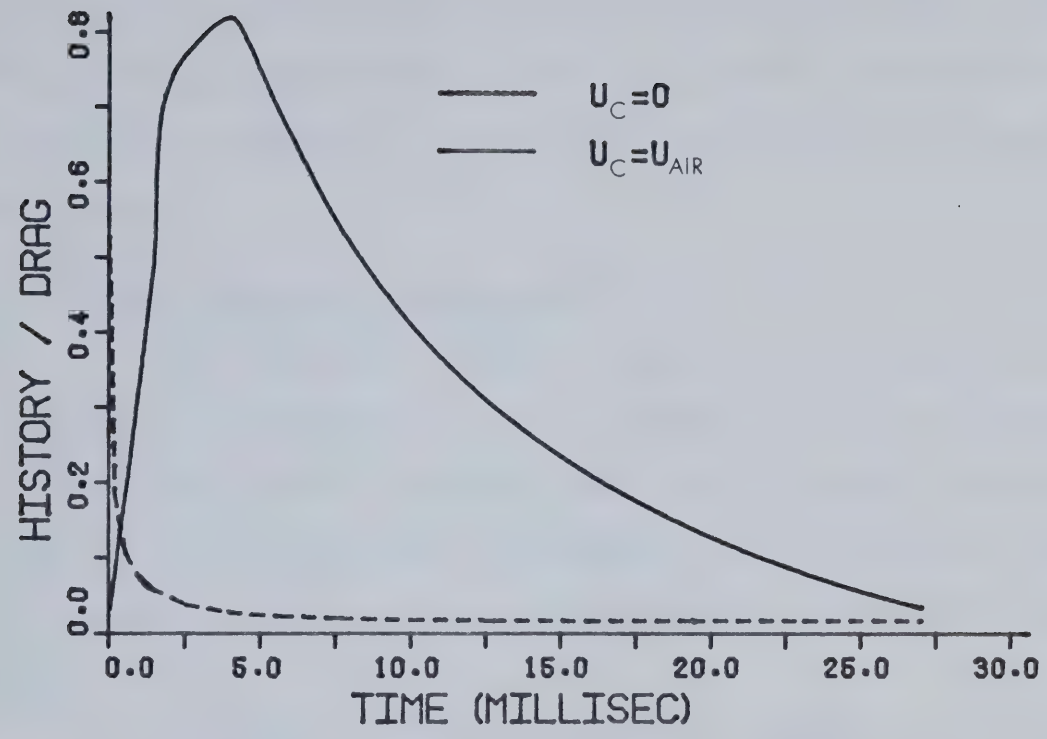

FIGURE 2.1a (TOP) and FIGURE 2.1b (BOTTOM) : Importance of the history term relative to the drag force as a function of injection velocity. The arrow in Figure 2.1b indicates the beginning of the working section.

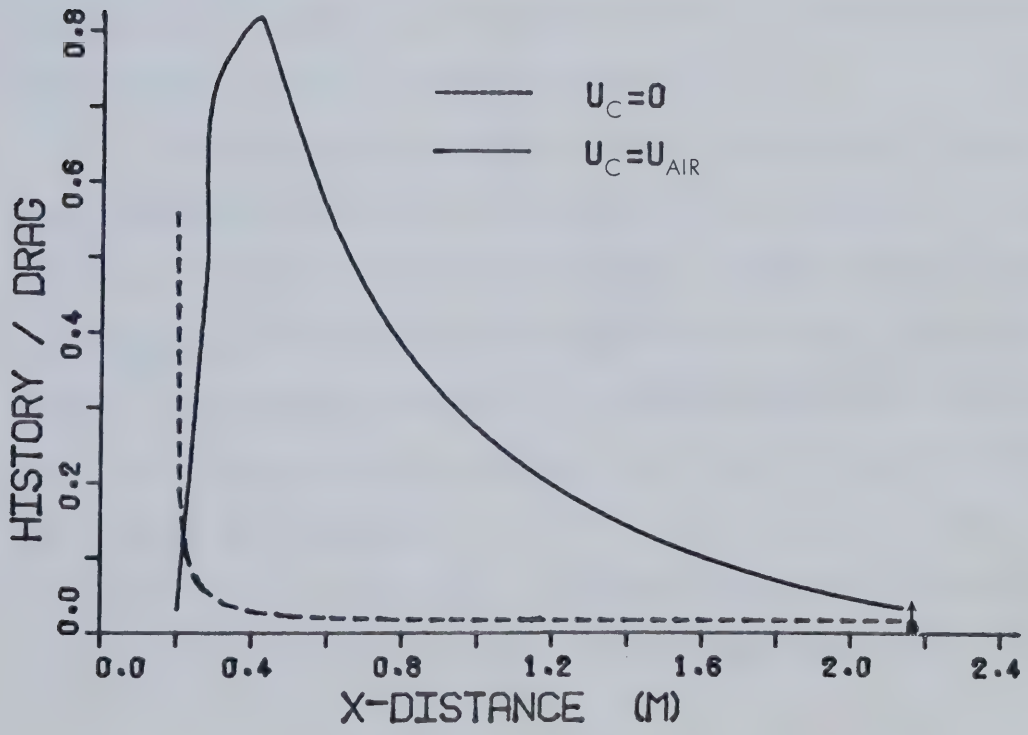

approaches a maximum of relative importance soon after injection from the sprayers. When the droplet is near the sprayers, the history term should not be neglected if the initial injection relative velocities are small.

2.5 Droplet Growth and Thermodynamics

When a pure water droplet is placed in an environment of humid (or dry) air, the droplet will grow or evaporate by the net diffusion of water vapor molecules towards or away from its surface. Associated with this diffusional growth is a substantial flow of heat to or from the droplet surface as a result of the release or absorption of latent heat.

Any attempt to solve the problem of diffusional growth by condensation must consider the droplet thermodynamic and growth equations simultaneously. The simplest case, which is treated in this section, describes the processes that control the growth of a droplet that is stationary with respect to the surrounding air. In the following section, the growth of a moving droplet is considered.

The assumptions considered in the single droplet and the droplet ensemble models are similar to those used by many authors in modeling diffusional growth. The simplified growth and thermodynamic equations that result have been derived by Pruppacher and Klett (1977), for example. In short, the principal assumption is radially symmetrical diffusion of vapor to or from a motionless droplet. Additional assumptions that are used include the following:

1. The gas that is immediately in contact with the droplet surface is in equilibrium with the droplet. Hence, the temperature and vapor

density fields immediately over the droplet surface are determined by the properties of the droplet.

2. The steady-state equations are used.

3. The droplet can be modeled as a rigid sphere of uniform temperature.

A further discussion of these assumptions and their validity for the present study is given in Section 2.7.

The forms of energy accounted for in this model include latent heat, the internal energy of the droplet, radiation, heat conducted to or from the droplet surface, and convection. The last term refers to the effect of droplet motion on the heat transfer and is discussed in the next section.

The rate of droplet growth in air is governed by the rate of transfer of water vapor between the droplet surface and the environmental air. Using the above assumptions, Pruppacher and Klett (1978, p. 414) formulate an equation for the mass rate of change of the droplet, dm_c/dt, due to mass diffusion. The steady-state result is,

$$\frac{dm_c}{dt} = 4\pi r_c^2 \rho_w \frac{dr_c}{dt} = 4\pi \mathscr{D} r_c (\rho_v - \rho_{v_c}) \qquad (2.5.1)$$

where $\mathscr{D}$ is the diffusivity of water vapor in air and ρ_v and ρ_{v_c} refer to vapor density fields at the droplet surface and in the distant (undisturbed) environment, respectively. It is assumed that the droplets are sufficiently far apart so that it is meaningful to refer to a distant undisturbed environment.

The latent heat, q, released by condensation at the droplet surface is given by

$$\left.\frac{dq}{dt}\right|_{\substack{\text{latent}\\\text{heat}}} = 4\pi \ell_v \mathscr{D} r_c (\rho_v - \rho_{v_c}) \qquad (2.5.2)$$

where the specific latent heat of vaporization is denoted as ℓ_v. If the Perfect Gas Law is applied, Equation 2.5.2 can be written as,

$$\left.\frac{dq}{dt}\right|_{\substack{\text{latent}\\\text{heat}}} = \frac{4\pi \ell_v \rho r_c}{R_v}\left(\frac{e}{T} - \frac{e_c}{T_c}\right) \qquad (2.5.3)$$

Following the rotation of the previous sections, e_c is the partial vapor pressure at the droplet surface and e is the partial vapor pressure of the undisturbed environment.

An expression for the process of thermal diffusion is formulated by Pruppacher and Klett (1978, p. 418) using mathematical arguments that are similar to those required to derive (2.5.1). The result describing the rate of heat loss by conduction is,

$$\left.\frac{dq}{dt}\right|_{\text{conduction}} = 4\pi r_c k(T_c - T) \qquad (2.5.4)$$

where k is the coefficient of thermal conductivity of moist air.

The heat loss by long wave radiation is obtained from the Stefan-Boltzmann Law (see, for example, Kern, 1950, p. 74) and is given by

$$\left.\frac{dq}{dt}\right|_{\text{radiation}} = 4\pi r_c^2 \sigma E(T_c^4 - T^4) \qquad (2.5.5)$$

where σ is the Stefan-Boltzmann constant and E is the emissivity of the water droplet. The effect of short wave radiation on the droplet thermodynamics is ignored.

The rate of change of the internal energy is written as,

$$\left.\frac{dq}{dt}\right|_{\text{internal}} = \frac{4}{3}\pi r_c^3 \rho_w c_w \frac{dT_c}{dt} + 4\pi c_w \rho_w T_c r_c^2 \frac{dr_c}{dt} \qquad (2.5.6)$$

where c_w is the specific heat capacity of liquid water.

Combining these terms, the energy balance equation for a stationary droplet growing in a motionless atmosphere is found from a balance of the internal energy, the latent heat, and the heat radiated and conducted from the droplet surface. The resulting heat balance equation is,

$$\frac{4}{3}\pi r_c^3 \rho_w c_w \frac{dT_c}{dt} = \frac{4\pi r_c \ell_v \alpha}{R_v}\left[\frac{e}{T} - \frac{e_c}{T_c}\right] + 4\pi r_c k(T-T_c)$$

$$+ 4\pi\sigma E r_c^2 (T^4 - T_c^4) \qquad (2.5.7)$$

where the second term on the right hand side of (2.5.6) is neglected relative to the latent heat term, $\ell_v \frac{dm_c}{dt}$.

The present study assumes that the pure water droplet exists in a supercooled state for droplet temperatures below 0°C. Experiments confirm, however, that there is a limit to the degree of this supercooling. Factors that affect the maximum supercooling include droplet size, the rate of cooling of the droplet, and the concentration of impurities (Willbanks, 1973, p.14). When droplet freeze-out (i.e. freezing of the droplet) occurs, the thermodynamic and growth equations must account for the changes that freeze-out produces in the specific heats, the energy flows, and in the liquid water contents (See Section 3.1). In a real test facility, droplet freeze-out may occur due to a contamination of the spray water with particles that cause ice nucleation. For the present study, the problem of droplet freeze-out is not considered. Given further continuation of this work, it is recommended that droplet freeze-out be included.

Before the droplet growth and thermodynamic equations can be integrated, it is necessary to write an expression for the equilibrium vapor pressure, e_c, at the droplet surface. (It is noted that the droplet

would not grow if the vapor pressure actually attained its equilibrium value.) An appropriate expression for vapor pressure is Kelvin's equation (see Neiburger and Chien, 1960). This equation accounts for the effect of the droplet curvature on the vapor pressure of a pure water droplet and is written as,

$$e_c = e_{sat}(T) \left[\exp\left(\frac{2\sigma'_{w/A}}{\rho_w r_c R_v T_c} \right) \right] \qquad (2.5.8)$$

The quantity $\sigma'_{W/A}$ refers to the surface tension of water in air and $e_{sat}(T)$ is the saturation vapor pressure with respect to a plane water surface. Both of these quantities may be calculated as functions of temperature. The quantity, $e_{sat}(T)$, is obtained from the Clausius-Clapeyron equation, which is discussed in Appendix D.

2.6 Ventilation Effects

If the air and the droplet are moving with respect to each other, the transfer of water vapor and heat between the droplet surface and the air is significantly enhanced by the motion of the air around the droplet. This ventilation effect results because parcels of air which are approaching the droplet temperature and vapor pressure by contact with the droplet surface are being removed continuously.

The customary approach to this problem is to introduce dimensionless quantities that characterize the forced convection into the expressions for heat and mass transfer. One quantity that is commonly used in the chemical engineering literature is a mean Sherwood number, $\overline{Sh}$. In the meteorological literature, the effect of ventilation is generally expressed by means of a mean ventilation coefficient, $\overline{f}$, defined by

$$\frac{dm_c}{dt} = \bar{f}\left(\frac{dm_c}{dt}\right)_0 \qquad (2.6.1)$$

where dm_c/dt is the evaporation rate of a moving droplet and $(dm_c/dt)_0$ is the evaporation rate of a stationary droplet. Since the mass flux will not be uniform over the ventilated droplet surface, a mean parameter $\bar{f}$ is used to characterize mass transfer from the droplet as a whole. The dimensionless quantities, $\bar{f}$ and $\overline{Sh}$, are related by the equation,

$$\bar{f} = \frac{1}{2}\overline{Sh}$$

If the droplet is stationary, (2.6.1) and (2.6.2) imply that $\bar{f} = 1.0$ or $\overline{Sh} = 2.0$.

Theoretical studies have had limited success in describing the effect of forced convection on the heat and mass transport from a spherical body. As a result, the relevant equations (Navier-Stokes, growth and energy equations) are usually solved by finite-difference techniques. A numerical solution to the problem is presented in a paper by Woo and Hamielec (1971), for example. These results are in excellent agreement with wind tunnel measurements of droplet evaporation by Beard and Pruppacher (1971). The values of $\bar{f}$ that were obtained by Beard and Pruppacher are closely approximated by the following empirical expression:

$$\bar{f} = \frac{\overline{Sh}}{2} = 1.00 + 0.108\,(Sc^{1/3}\,Re^{1/2})^2,$$

$$\text{for} \quad Sc^{1/3}\,Re^{1/2} \leq 1.4$$

and,

$$\bar{f} = \frac{\overline{Sh}}{2} = 0.78 + 0.308\,(Sc^{1/3}\,Re^{1/2}),$$

$$\text{for} \quad Sc^{1/3}\,Re^{1/2} \geq 1.4 \qquad (2.6.2)$$

The dimensionless ratios used in (2.6.2) are the Schmidt number, $Sc = \nu/\mathscr{D}$, and the droplet Reynolds number, Re. The last relation is valid for

$Sc^{1/3}Re^{1/2} < 16$, which roughly corresponds to flow with Re < 320.

The conventions that exist in the literature for describing the Sherwood number are often ambiguous since many of these definitions are based on experimental or theoretical convenience. The Sherwood number used in this study is defined by Beard and Pruppacher on the basis of experimental convenience and is given by the relation,

$$\frac{dm_c}{dt} = \frac{4\pi r_c \mathcal{D}_f}{1-e_f/P} \frac{(e_c-e)}{R_v T_f} \frac{\overline{Sh}}{2} \qquad (2.6.3)$$

The above expression introduces the quantities,

$$T_f = \frac{T_c + T}{2}, \quad e_f = \frac{e_c + e}{2}, \quad \text{and} \quad \mathcal{D}_f = \mathcal{D}(T_f)$$

which are respectively the mean or "effective" values over a vapor transfer path of the temperature, vapor pressure and diffusivity of water vapor.

The effect of ventilation on the transfer of heat from the droplet surface by conduction must be considered. By analogy with (2.6.2) a dimensionless number characterizing the heat transfer , the mean Nusselt number, $\overline{Nu}$, is introduced. The rate of heat loss due to conduction and convection is given by

$$\left.\frac{dq}{dt}\right|_{\substack{\text{conduction} \\ \text{and convection}}} = 4\pi r_c k(T_c - T) \frac{\overline{Nu}}{2} \qquad (2.6.4)$$

The expression for the mean Nusselt number is similar to the expression for the mean Sherwood number. The mean Nusselt number is written in terms of the Reynolds number and the Prandtl number. The Prandtl number, $Pr = \nu/\kappa$, is analagous to the Schmidt number and is

obtained by replacing the diffusivity of water vapor in the Schmidt number by the thermal diffusivity of air, $\kappa = k/(\rho c_p)$. The mean Nusselt number is

$$\frac{\overline{Nu}}{2} = 1.00 + 0.108\ (Pr^{1/3}\ Re^{1/2})^2, \quad \text{for} \quad Pr^{1/3}\ Re^{1/2} \leq 1.4$$

and,

$$\frac{\overline{Nu}}{2} = 0.78 + 0.308\ (Pr^{1/3}\ Re^{1/2}), \quad \text{for} \quad Pr^{1/3}\ Re^{1/2} \geq 1.4 \qquad (2.6.5)$$

The last relation is valid for $Pr^{1/3}Re^{1/2} < 16$ or roughly for flow with $Re < 320$.

If the effects of ventilation described by (2.6.3) and (2.6.4) are introduced into Equation 2.5.7, a thermodynamic equation is obtained for the moving droplet. The relation is,

$$\frac{4}{3}\pi r_c^3 \rho_w c_w \frac{dT_c}{dt} = \frac{4\pi r_c \ell_v \rho_f}{R_v}\left[\frac{e}{T} - \frac{e_c}{T_c}\right]\frac{\overline{Sh}}{2} + 4\pi r_c k(T-T_c)\frac{\overline{Nu}}{2}$$

$$+ 4\pi\sigma E r_c^2 (T^4 - T_c^4) \qquad (2.6.5)$$

The growth equation for the moving droplet is given by (2.6.3). Using (2.4.4), (2.6.3), and (2.6.6), the system of equations describing droplet motion in an accelerating air flow can then be solved numerically.

2.7 Discussion of Assumptions

If the results of any model are to be useful, the assumptions that are applied must be realistic. With this objective in mind, this section evaluates the validity of some of the assumptions that are applied to this model. The same assumptions that describe droplet behavior are used in the ensemble model.

It was mentioned in Section 2.4 that significant errors may result when steady-state relations are used to predict the motion of a droplet that accelerates rapidly in a high speed air flow. For such cases, a number of non-steady state processes (that include the time dependent history term) should be considered. For example, observations indicate that the drag of the air on large water drops, characterized by a $Re \geq 300$, progressively increases with Reynolds number above that for rigid spheres. This increase in drag is attributed to three processes -- oscillation of the drops, generation of internal circulations, and distortion of the drop shape from spherical. These processes, which are important for large drops, may also be important for smaller droplets when their accelerations (and relative velocities) are large.

The assumption that water droplets can be modeled as rigid spheres is justified for steady-state motion with $Re \leq 200$ (LeClair et al., 1969). This corresponds roughly to droplets with radii less than 450 microns. For non-steady state motion (large droplet accelerations), it is expected that greater surface stresses will result in a flattening of the droplet. As a result, the properties predicted by the drag, growth, and thermodynamic equations, which model the droplet as a rigid sphere, become inaccurate.

The existence of an internal circulation inside falling drops is supported by many experiments. For a complete description of this effect and the effect of oscillations on drop motion, the reader is referred to Pruppacher and Klett (1978, p. 305-328). In short, past investigations indicate that the contribution of internal circulations to the increase in the drag is negligible compared to the contribution from distortion in the drop shape. The importance of vibration to the

drag depends upon its effect on the drop shape.

Detailed discussions of the assumptions needed to derive the steady-state growth and thermodynamic equations can be found in several studies. Some conclusions based on these studies are considered below.

1. The time dependent solution to the problem of water vapor diffusion to a sphere (Borovikov et al., 1961) shows that the steady-state diffusional growth relation (2.5.2) can be used when the droplets are smaller than 100 microns in radius. Pruppacher and Klett (1978, p. 414) calculate that the steady-state description is not valid when significant changes in the ambient vapor field occur during droplet travel times less than a critical time, $t_{crit} = r_c^2/(\pi \mathcal{D})$. The time, t_{crit}, is an estimate of the time that is required to establish steady-state diffusion if the droplet is growing in an undisturbed environment. For T = 0°C and P = 1 atmosphere, the calculations indicate that $t_{crit} \leq 1.7$ microseconds for droplets with a radius smaller than 100 microns. Since the thermal diffusion problem is analagous to the mass diffusion problem and $k \approx D$, Pruppacher and Klett estimate that the steady-state thermal relations may also be used if significant changes in the ambient air temperature do not occur during droplet travel times less than t_{crit}.

   For the present study, changes in the ambient air properties occur on a time scale of milliseconds so that steady-state relations may be used.

2. It is customary to assume that the droplet has an isothermal surface because of the large thermal conductivity of water and because it is expected that small differences will exist in the heat flux around the drop surface (Ibid., p. 444). Contrary evidence from studies

showing that the ventilation effect has a strong local variation over the droplet surface suggest, however, that there must be a non-zero temperature gradient at the droplet surface, although the gradient will be somewhat degraded by the droplet internal circulation. For lack of information on this point, it is usually assumed that the droplet has an isothermal surface.

3. The assumption that the moist air is a continuous field right up to the droplet surface is unrealistic for droplets with radii comparable to a mean free path of vapor molecules in air. The molecular exchange processes that occur at the liquid-vapor surface can be incorporated into a modified growth theory (Fukuta and Walter, 1970) using results from kinetic theory. Since the modified equations become complicated to parameterize and to solve, these molecular effects are not considered in the present study. It is emphasized though, that errors may be introduced when the molecular processes are neglected. A study by Fitzgerald (1972, p. 132), for example, calculates that the instantaneous growth rates for a 10 micron radius droplet are reduced to roughly one-half of the growth rates that are calculated when these corrections are ignored.

Finally, the assumption of a one-dimensional isentropic flow for moist air is valid only when heat sources and sinks are absent and when frictional forces and flow turbulence are ignored. The validity of these assumptions depends upon the operating conditions of the tunnel considered.

CHAPTER 3

THE DROPLET ENSEMBLE MODEL

3.1 The System

The closed system (portion of matter) treated by the droplet ensemble model consists of two subsystems -- moist air and an ensemble of water droplets. Unlike the case of the single droplet model, the equations of the ensemble model account for the contributions of the droplets to the total energy, momentum, and mass of the system.

For the ensemble model, as for the single droplet model, we consider the matter within a volume contained by the contraction and working sections of the tunnel, beginning at the location of the sprayers ($x = 0.2m$). Heat transfer and frictional dissipation at the tunnel walls are assumed to be negligible and steady-state assumptions apply. It is also assumed that the air flux injected with the water droplets is negligible relative to the air flux that would result without the nozzles. An estimate of this flux for flow in the NRC tunnel is given in Appendix C. The results indicate that its contribution is negligible.

Although a realistic drop size distribution for the spray is described by a range of droplet sizes, the present model is simplified by treating an ensemble of N identical spherical droplets per unit volume. Each droplet is characterized by a temperature T_c, its radius r_c, and a velocity U_c. The droplet velocity is measured in a frame of reference that is fixed to the tunnel walls. The droplets are injected parallel to the air flow and the droplets are assumed to be uniformly distributed across any cross-section of the tunnel. Furthermore, it is convenient to regard the droplets as a pseudo-continuum so that an average droplet density

(mass of droplets per unit volume of the air-spray mixture) may be defined. The droplets are described by the mass density, ρ_c,

$$\rho_c = \frac{4}{3} \pi r_c^3 \rho_w N$$

When droplet evaporation or condensation occurs, the mixing ratio of the moist air will not remain constant. Although vapor is continuously introduced or depleted by droplet evaporation or condensation, it is assumed that the moist air is well-mixed at all times and that the moist air can be characterized by a uniform temperature, T, and a velocity, U.

It is emphasized that the "well-mixed vapor" assumption is not realistic for tunnels where the time that is characteristic of the droplet motion compares to a time characteristic of the mixing, τ_m. If it is assumed that turbulent mixing processes dominate over the molecular processes, a characteristic time for the mixing is,

$$\tau_m = \frac{L^2}{K_e}$$

where K_e is the coefficient of eddy diffusivity and L is a scale or characteristic width of the tunnel. An estimate of the time characteristic of the motion is given by,

$$\tau_a = U / \left(\frac{dU}{dt}\right)$$

For flow in tunnels where $\tau_a \leq \tau_m$, (i.e. large droplet accelerations), adequate mixing cannot occur and the vapor associated with droplet evaporation or condensation is not at the same temperature or velocity as the surrounding well-mixed air.

When the droplets are identical, the droplet growth, thermodynamic, and drag equations of the single droplet model describe the motion and growth of the ensemble. Since the equations describing the flow of the moist air and droplets are coupled, the properties of the air and droplets are obtained by simultaneously solving the droplet equations (2.4.4, 2.5.1, 2.5.7) and the global conservation equations. The global equations include two relations that describe the coupling of momentum and entropy. In addition, the mass continuity equations for the water substance and for the dry air are required.

The problem of the coupled motion can be considered with respect to a control volume fixed in space (Eulerian frame of reference). Consider the volume, V, sketched in Figure 3.1. This control volume of thickness, δx, is bounded by the cross-sectional areas $A_1 = A(x)$ and $A_2 = A(x + \delta x)$ and by the lateral surface, A_3, which coincides with the flow boundary of the system. The steady-state integral equation for the mass, energy, and momentum flow through the control volume are determined by applying Reynolds Transport Theorem to the matter within the volume (Crowe, 1976, p. 387). The theorem states that the rate of accumulation of some extensive property (mass, entropy, energy) in a closed system is equal to the rate of increase of the property in the control volume plus the net influx of the property across the control surface for the very instant that the matter occupies the control volume. Mathematically, the theorem is written,

$$\frac{DQ}{Dt} = \frac{\partial}{\partial t}\int_{\upsilon} \rho q \, d\upsilon + \int_{S} \rho q \vec{U} \cdot d\vec{A} \qquad (3.1.1)$$

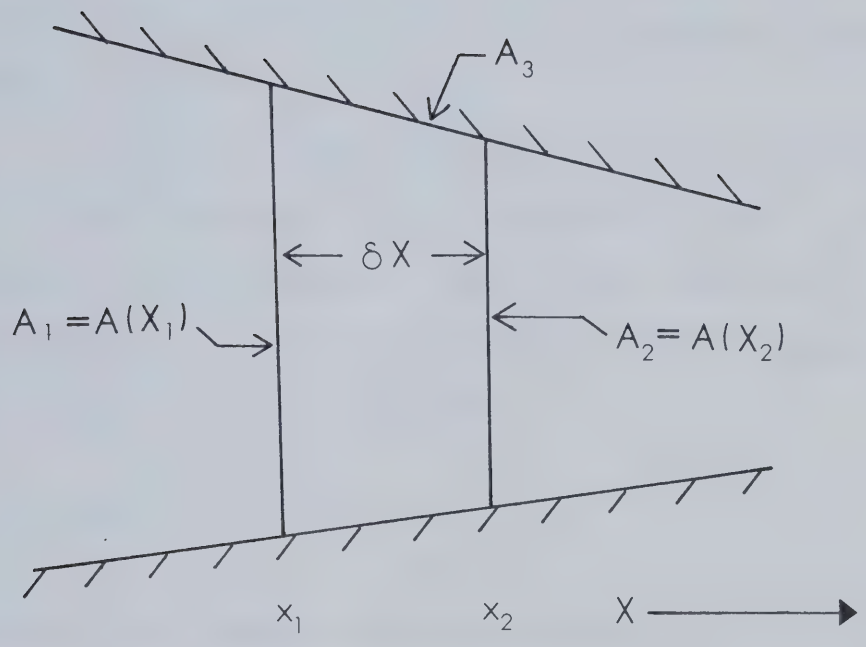

FIGURE 3.1 : A control volume bounded by the cross-sectional areas, A_1 and A_2, and the lateral surface, A_3.

where $\frac{DQ}{Dt}$ is the total time derivative of some extensive quantity, Q, and the specific quantity, q = DQ/Dm. The thickness, δx, is determined by the requirement that significant changes in the averaged properties should not occur on a scale that is smaller than the length, δx. The scale of these significant changes is considered to be large relative to the scale of local changes (i.e. mean free path). Thus, the control volume must contain many droplets in order to define an average droplet velocity or temperature, for example.

The mass continuity equation for the water substance in the control volume must account for the total water content of the droplet ensemble and of the moist air. Since not only steady-state is assumed, implying $\partial m_w/\partial t = 0$, but also conservation of water substance is assumed, implying $Dm_w/Dt = 0$, it follows that,

$$\int_S (\rho_c \vec{U}_c + \rho_v \vec{U}_v) \cdot d\vec{A} = 0$$

In addition, it is assumed that mass transfers do not occur at the lateral surface, A_3, of the control volume. The steady-state mass continuity equation for the water substance that is obtained by applying Reynold's Theorem is,

$$\rho_{v_1} U_1 A_1 + \rho_{c_1} U_{c_1} A_1 = \rho_{v_2} U_2 A_2 + \rho_{c_2} U_{c_2} A_2 \qquad (3.1.2)$$

In addition to mass continuity, the number of droplets crossing a cross-sectional area must be conserved. Thus, steady-state changes in the mass of the liquid water substance occur only by evaporation or condensation of a constant number flux of the droplets. The continuity equation for the number of droplets is written,

$$N_1 U_{c_1} A_1 = N_2 U_{c_2} A_2 \qquad (3.1.3)$$

3.2 The Global Entropy Equation

Application of the Second Law of Thermodynamics is simplified for a coupled air and water system if specific entropy is used. Specific entropy is a well-defined thermodynamic property for each component of the system when an equilibrium state exists or when reversible changes in its state occur. Iribarne and Godson (1973, p. 75), for example, derive an expression for the entropy of a closed two-phase system consisting of dry air, liquid water, and its saturated vapor. The entropy equation is written in terms of two other thermodynamic or state variables, which are taken to be temperature and pressure.

In Appendix D, an approximation is derived for the entropy of a system consisting of dry air, water vapor, and liquid water in the form of droplets. The derivation assumes that the temperatures of the moist air and droplets are all equal and that the vapor pressure of the moist air is the equilibrium vapor pressure defined with respect to a curved droplet surface. The resulting entropy equation is an approximation since the equilibrium vapor pressure of the droplets is replaced by the saturation vapor pressure defined with respect to a plane surface. Calculations for a 10 micron droplet at a temperature of 20°C indicate that droplet curvature increases the equilibrium vapor pressure above the saturation vapor pressure by a factor of 1.000086.

The present system, where the moist air and the droplets move with respect to each other, is not characterized by an equilibrium state since the temperatures of the moist air and droplets can differ from one another and the partial vapor pressure of the moist air can depart

significantly from the droplet equilibrium vapor pressure. For such a nonequilibrium open system in which irreversible processes are occuring (i.e. entropy is not conserved), the laws of classical thermodynamics provide a set of inequalities describing the direction of the changes in its state.

If it is assumed that the entropy within a control volume remains constant, an entropy equation may be derived that describes the state of the coupled air and droplet flow. As in the first model, the derivation requires that frictional forces and tunnel turbulence be ignored and that the tunnel walls are insulated. The validity of these assumptions depends upon the operating conditions of the tunnel considered. The constant entropy assumption also means that phase changes between the air and the spray are reversible.

The result of these derivations for the steady-state flow, given in Appendix E, is that the total entropy flux crossing a cross-sectional area of the tunnel is constant. The constant entropy flux is given by,

$$\rho_d UA(c_{pd}\ell nT - R_d\ell nP_d) + \rho_v UA\left[\frac{\ell_v(T)}{T} - R_v\ell n\frac{e}{e_{sat}(T)}\right]$$

$$+ \rho_v UAc_{pv}\ell nT + \rho_c U_c Ac_w\ell nT_c = \text{constant} \qquad (3.2.1)$$

3.3 The Global Momentum Equation

When the droplets and moist air have different velocities, any phase changes will result in a change of the momentum of the system. The integral (area averaged) momentum flux for the steady-state flow of the moist air and droplets is determined by applying Newton's Second Law of Motion and the Reynolds Transport Theorem to the control volume

(see Figure 3.2).

"The net force acting on the material within the control surface is equal to the increase of momentum flux of the streams flowing through the control surface". (Shapiro, 1953, p. 224). The forces that combine to produce the momentum changes are:

1. the pressure forces at the end cross-sectional areas where such pressure differences tend to increase the speed of the moist air;
2. the distributed pressure forces exerted by the tunnel walls on the fluid and producing the required changes in the direction of the flow;
3. the drag force exerted by the droplets on the air.

Considering the x-component of the pressure forces acting on the internal surfaces of the control volume, the net force acting on the cross-sectional areas, A_1 and A_2, is $(P_1A_1 - P_2A_2)$. Since the x-component of the distributed pressure forces acting on the bounding surface A_3 is difficult to determine, an average pressure, $\bar{P} = (P_1 + P_2)/2$, is used. This approximation is valid for a control volume where the x-component of pressure varies linearly (or more slowly) with the x-distance. Referring to Figure 3.2, the <u>distributed</u> pressure force is,

$$\hat{i} \cdot \int P \, dS \, \hat{n} \approx - \bar{P} \int dA = \bar{P} (A_2 - A_1)$$

where dA is the projection of an element of the lateral surface on to a cross-sectional plane, $\hat{i}$ is a unit vector in the positive x-direction and $\hat{n}$ is the inward unit vector normal to the lateral surface. The net pressure force acting on the matter within the control volume is,

$$P_1A_1 - P_2A_2 = \bar{P} (A_1 - A_2) = \bar{A} (P_1 - P_2) \qquad (3.3.1)$$

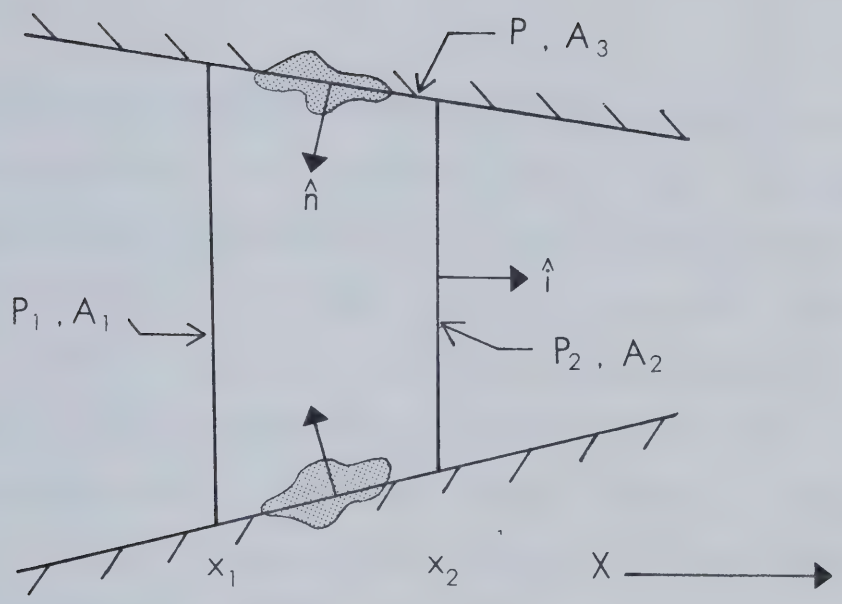

FIGURE 3.2 : Pressure force acting on a control volume. The unit vector in the x-direction is $\hat{i}$, and $\hat{n}$ is the unit vector normal to the lateral surface, A_3.

The steady-state drag exerted by the droplets on the air for a unit volume of the system is given as,

$$F_{drag/volume} = N\left[6\pi r_c \mu (U-U_c)(1+\alpha Re^{\beta})\right] \qquad (3.3.2)$$

In this study, the momentum transfer of the droplets to the air may be neglected relative to the pressure gradient force. Calculations using the accelerations obtained from the single droplet model for flow of a 10 micron droplet in the NRC high speed icing tunnel indicate that the ratio of the drag force to the pressure gradient force for 2.4×10^9 droplets per cubic meter should be less than 10^{-2}. Thus, the momentum changes that are associated with the phase changes are negligible.

The net one-dimensional momentum flux of the streams flowing through the control volume may be written as,

$$\left[\rho_d U^2 A + \rho_v U^2 A + \rho_c U_c^2 A\right]_{x=x_1} - \left[\rho_d U^2 A + \rho_v U^2 A + \rho_c U_c^2 A\right]_{x=x_2}$$

$$= \text{momentum flux} \qquad (3.3.3)$$

Using this result and neglecting the drag and gravitational terms, the momentum equation is,

$$\left[\rho_d U^2 + \rho_v U^2 + \rho_c U_c^2\right]_{x=x_1} A_1 - \left[\rho_d U^2 + \rho_v U^2 + \rho_c U_c^2\right]_{x=x_2} A_2$$

$$= \bar{A}\,(P_1 - P_2) \qquad (3.3.4)$$

CHAPTER 4

DISCUSSION OF RESULTS FOR NRC HIGH SPEED ICING TUNNEL

4.1 The Approach

In this chapter, the results obtained by modeling the flow through the contraction and working sections of the NRC high speed icing tunnel are reported and discussed. A parametric study is performed in order to determine the influence of initial conditions on the flow properties at the working section. For the duct geometry of the NRC high speed icing tunnel (discussed in Section 1.3), the following duct inlet properties are varied:

1. the moist air thermodynamic and kinetic state variables at the plenum (such as pressure, temperature, relative humidity and air speed);
2. the liquid water content of the spray at the sprayers;
3. the water injection velocity and temperature; and
4. the droplet radius.

Baseline values of these variables are selected and each of the inlet properties is varied one at a time. The following baseline values of the initial parameters are used:

liquid water content of spray	$10 g/m^3$
spray temperature	20°C
representative radius	25 microns
spray injection velocity	3 m/s
air speed at plenum	18.2 m/s
air temperature at plenum	2.22°C
relative humidity at plenum	50%

For an initial or plenum air velocity of 18.2 m/s, a high speed air flow is described for the NRC icing tunnel. The downstream air velocity at the working section is near 120 m/s. The air temperature, which is initially 2.22°C, decreases to a value near 1°C at the sprayers and has a value of -4.8°C at the working section. The distance from the plenum to the sprayers is 0.2 m and the distance from the plenum to the working section is 2.1336 m.

The spray velocity increases rapidly during the first 0.2 m of the contraction distance from the sprayers and approaches the air velocity. The downstream spray velocity at the working section is near 106 m/s, indicating that it lags the air velocity by 14 m/s. For an illustration of the variation of the temperatures and velocities of the spray and air with the contraction distance, the reader is referred to the upper curves of Figures 4.11 and 4.12. It is emphasized that the plenum velocity in these Figures is 20 m/s rather than 18.2 m/s (which is taken as the baseline value).

The reason for choosing the liquid water content of the spray to be 10 g/m^3 rather than a lower value more realistic of natural icing conditions (in the range of 0.5-2 g/m^3) is because it is desirable to observe the maximum coupling effect of the droplets and the moist air. The droplet radius is also chosen larger than a more representative value of say, 10 microns. Since larger droplets cool more slowly than smaller droplets, the choice of a larger baseline droplet radius means that axial variations of other properties are then better observed. The choice of a spray temperature of 20°C is determined from the fact that the spray water is usually kept at room temperature. The air that is injected with the droplets is heated to approximately 30°C to preclude freezing of the droplets on or within the sprayers. Although a typical cloud

environment is saturated, the baseline relative humidity for this icing simulation is taken as 50 percent. If a plenum relative humidity is chosen near saturation, the calculated relative humidities rise to large supersaturation values near the working section of the tunnel. (with relative humidities approaching 150 percent). In a real icing tunnel, contamination of the moist air with particles would limit the supersaturation.

The results described in this chapter are obtained under an assumption that the droplet disrribution consists of N identical droplets. A study by Willbanks and Shultz (1973) compared the effect on the downstream spray properties of mathematically simulating the water spray cloud with a realistic size distribution of droplets to the effect of simulating the cloud with a single droplet size. The single droplet size was equal to the mass median radius of the distribution. The mass median radius is defined as the radius of those droplets for which one-half of the entire liquid water content in the spray is contained in droplets whose radius is less than this median value. The distribution used was a measured distribution determined from a laser holography technique. The size distribution of their study was fairly similar to the size distributions found in cumuliform clouds. The results from their calculations indicated that the spray temperature was not highly dependent on wheth r the spray cloud was characterized by having a distribution of droplet sizes or a single uniform droplet size. It was concluded that, for typical icing conditions, the characterization of the icing conditions by a liquid water content and a mass median radius is sufficiently accurate for testing purposes.

The results of the parametric study are discussed in the following sections. For a discussion of the details of programming the two models, the reader is referred to Appendix H. Values of constants and physical relations needed to calculate some of the intermediate variables used in the dynamical and thermodynamical equations are given in Appendix G.

4.2 The Effect of Variation of the Plenum Relative Humidity

The effect on the spray temperature of a variation in the plenum relative humidity from 0 to 100 percent is shown in Figure 4.1. As the Figure indicates, the spray temperature is highly dependent upon the tunnel relative humidity. Thus, evaporation and condensation at the droplet surface play a major role in determining the spray temperature. By controlling the plenum relative humidity, the rate of mass transfers and consequently, the spray temperature at the working section may be controlled.

The calculations indicate that the moist air temperature and velocity are effectively independent of the tunnel relative humidity. The explanation is that the water vapor is only a small part of the mass flow of the air.

Figure 4.2 shows the effect that a variation in the plenum relative humidity has on the temperature difference between the spray and the air. It is seen in this Figure and in Figure 4.1 that the spray cools at a slower rate for the higher relative humidities since the droplet evaporation is less. When the plenum relative humidity is greater than 50 percent, Figure 4.2 indicates that the spray temperature lags

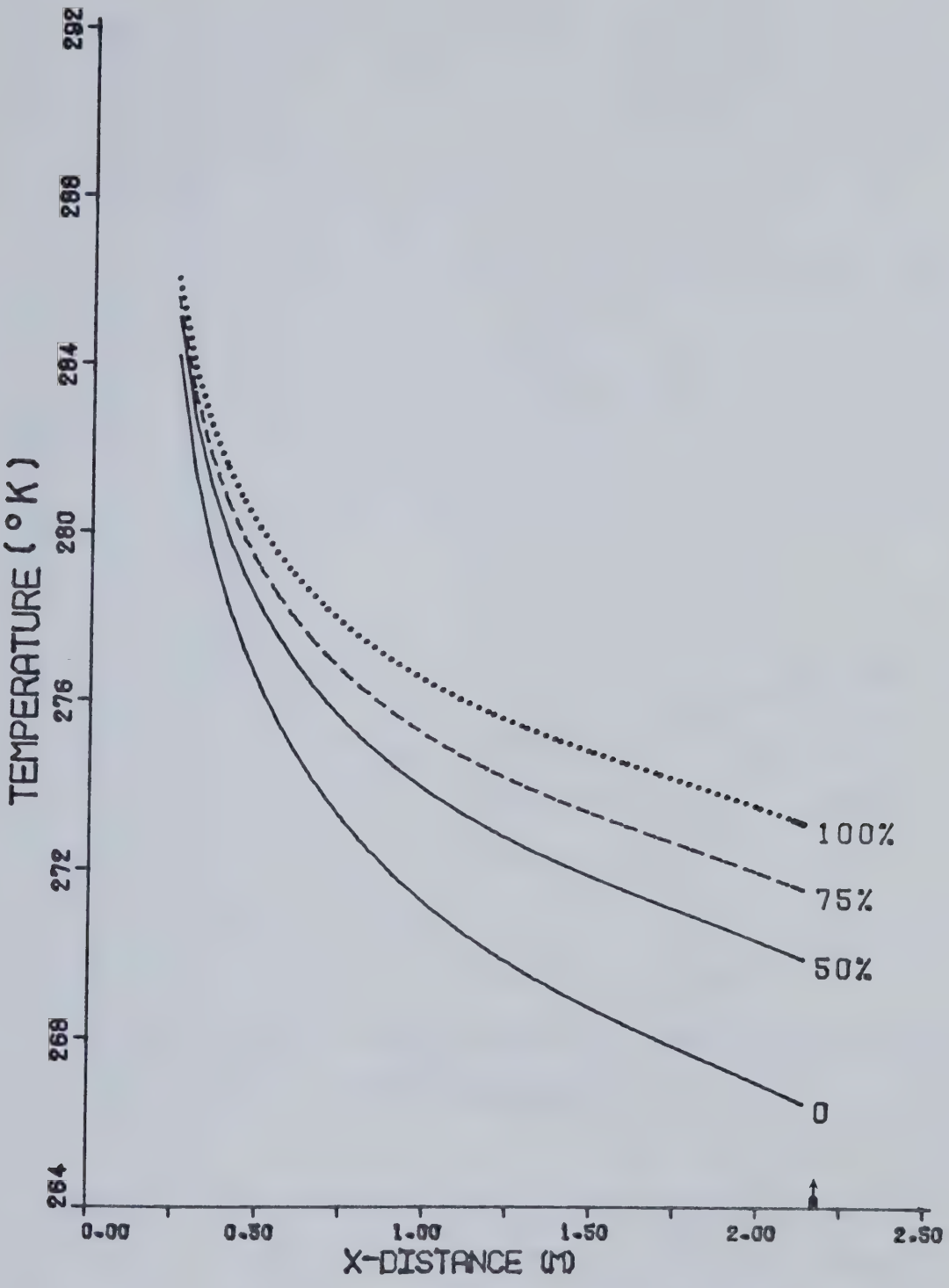

FIGURE 4.1 : The effect of initial relative humidity on the spray temperature as a function of distance from the plenum. The arrow indicates the beginning of the working section.

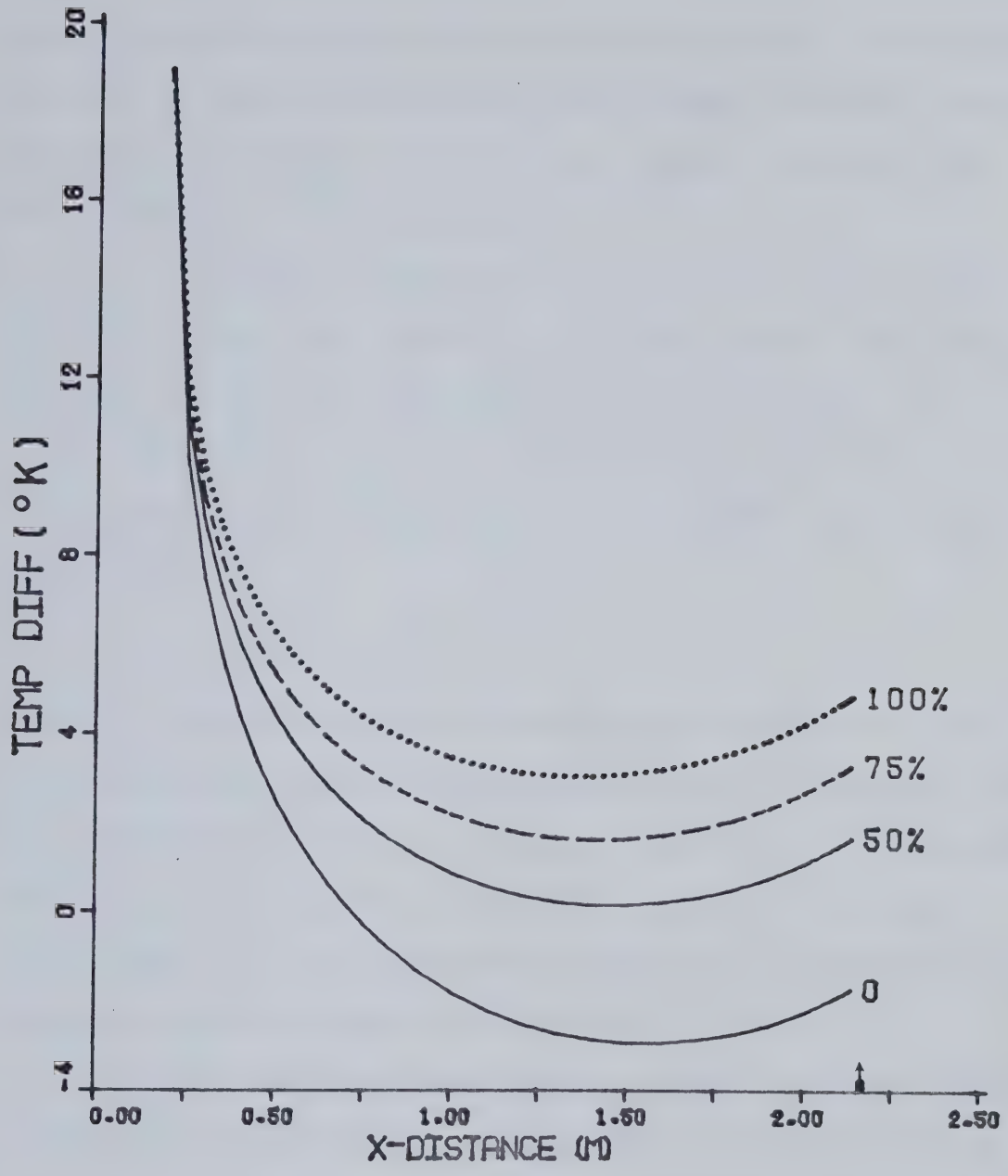

FIGURE 4.2 : The effect of tunnel relative humidity on the temperature difference (T_c-T) between the spray and air as a function of distance from the plenum. The arrow indicates the beginning of the working section.

the air temperature for the entire contraction distance. For the case where the air flow is initially dry at the plenum, the droplet evaporation is greatest and the spray actually becomes cooler than the air flow before reaching the working section.

It is suggested here that the temperature of the droplets approaches the wet-bulb temperature as the spray velocity approaches the air velocity. The wet bulb temperature, T_w, is defined (Rogers, 1976, p. 21) as "the temperature to which air may be cooled by evaporating water into it at constant pressure until saturation is reached". From the approximation (Ibid, p. 22),

$$\frac{T - T_w}{r_{sat} - r} = \frac{\ell_v}{c_p}$$

where r_{sat} is the mixing ratio corresponding to saturation of the air , it is seen that the wet-bulb temperature of the air increases as the mixing ratio and temperature of the air increase. When the relative humidity of the air is less than 100 percent and $r < r_{sat}$, it follows that $T_w < T$. When the relative humidity is greater than 100 percent (super-saturation), the approximation implies that $T_w > T$.

Unless the air is saturated, the air and spray (i.e. droplet) temperatures will be different. For low relative humidities, it is reasonable to expect the drop temperature to become cooler than the air temperature since $T_w < T$. When the moist air is saturated at the plenum, on the other hand, the tunnel relative humidity rises above 100 percent for the flow along the contraction section. (This effect is largely the result of the decrease in the air temperature). Since $T_w > T$ in this case, the droplet temperature can be expected to lag the temperature of the air (i.e. the droplet temperature exceeds the air temperature).

Hence, the relations shown in Figure 4.2 are explained if the droplet temperature tends to approach the wet-bulb temperature of the air.

4.3 The effect of Variation of the Liquid Water Content

Figure 4.3 indicates that a variation in the liquid water content of the spray has only a small effect on the temperature of the droplets. The Figure compares the effect of introducing a large liquid water content of $50g/m^3$ to that of having a negligible liquid water content. Calculations show that the liquid water content also has a very small influence on the temperature and velocity of the air. As shown in Figure 4.4, the temperature difference between the spray and the air does not vary significantly with the liquid water content. In short, these results indicate that there is no significant thermal feedback between the spray and the moist air. The reason for this small effect is that only a small quantity of water is sprayed into the tunnel relative to the mass flow of the air. It should be emphasized that this conclusion applies only for the small liquid water contents typical of icing simulations.

The solutions given by the single droplet model and by the ensemble model are, for practical purposes, identical. The advantage of using the ensemble model here if that the CPU time required to run the ensemble model on the AMDAHL 470 V/7 at the University of Alberta is roughly two-thirds of the time required to run the single droplet model.

4.4 The Effect of Variation of Initial Spray Temperature

Figure 4.5 indicates that the initial spray temperature has only a small effect on the final spray temperature of the working section. It is also seen in Figure 4.6 that the final temperature difference between

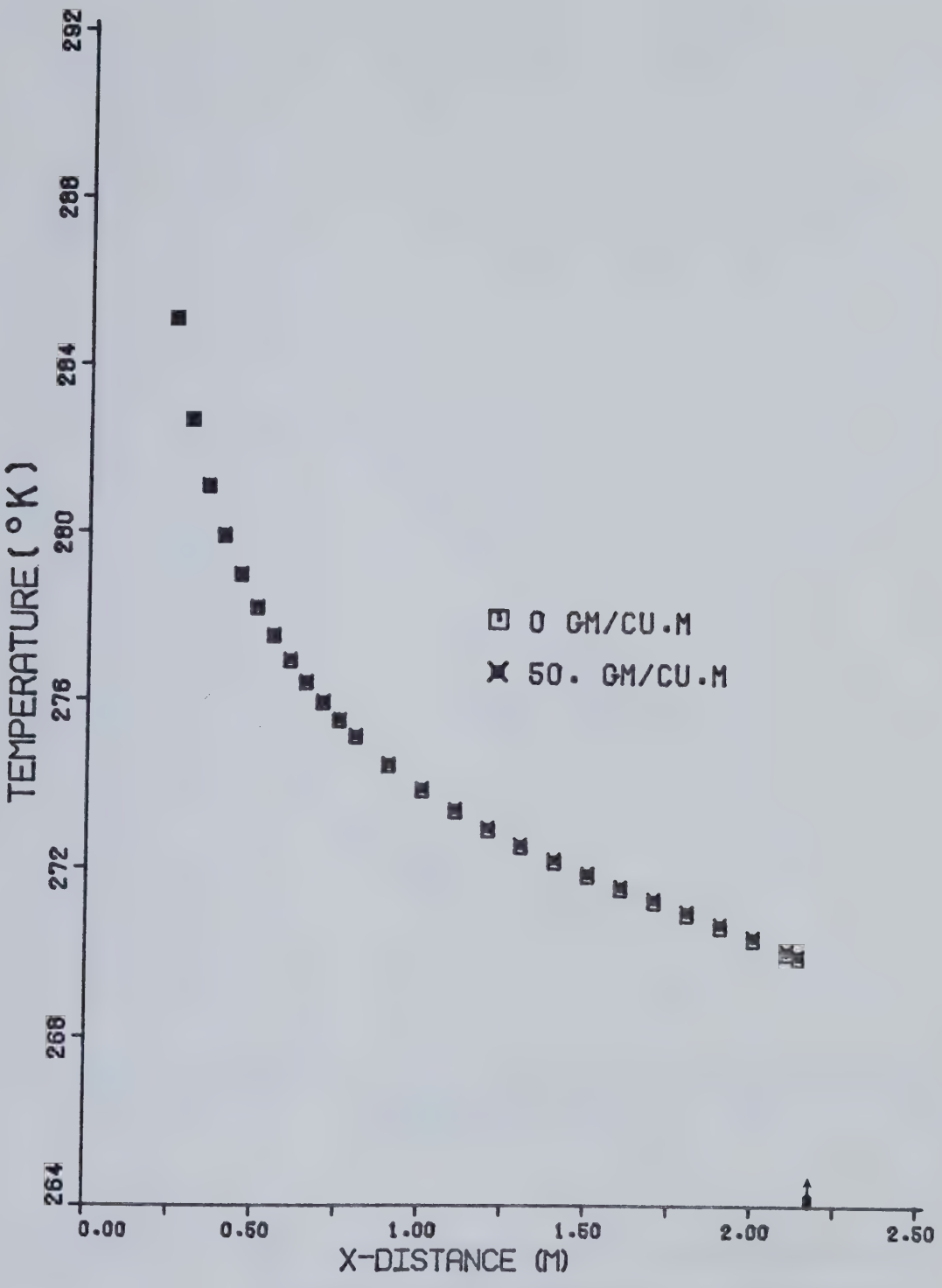

FIGURE 4.3 : The effect of initial spray liquid water content on the spray temperature as a function of distance from the plenum. The arrow indicates the beginning of the working section.

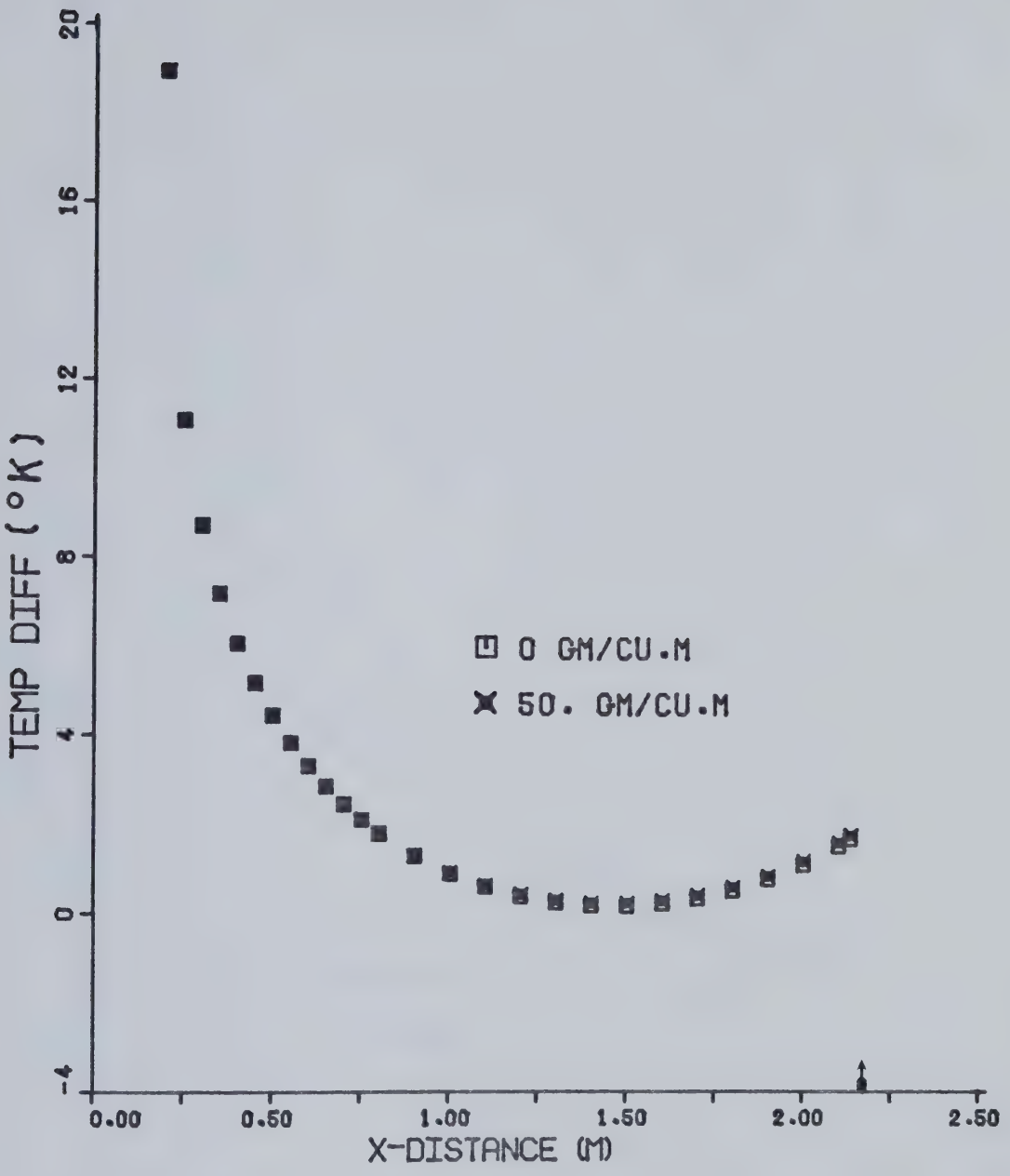

FIGURE 4.4 : The effect of initial spray liquid water content on the temperature difference (T_c-T) between the spray and air as a function of distance from the plenum. The arrow indicates the beginning of the working section.

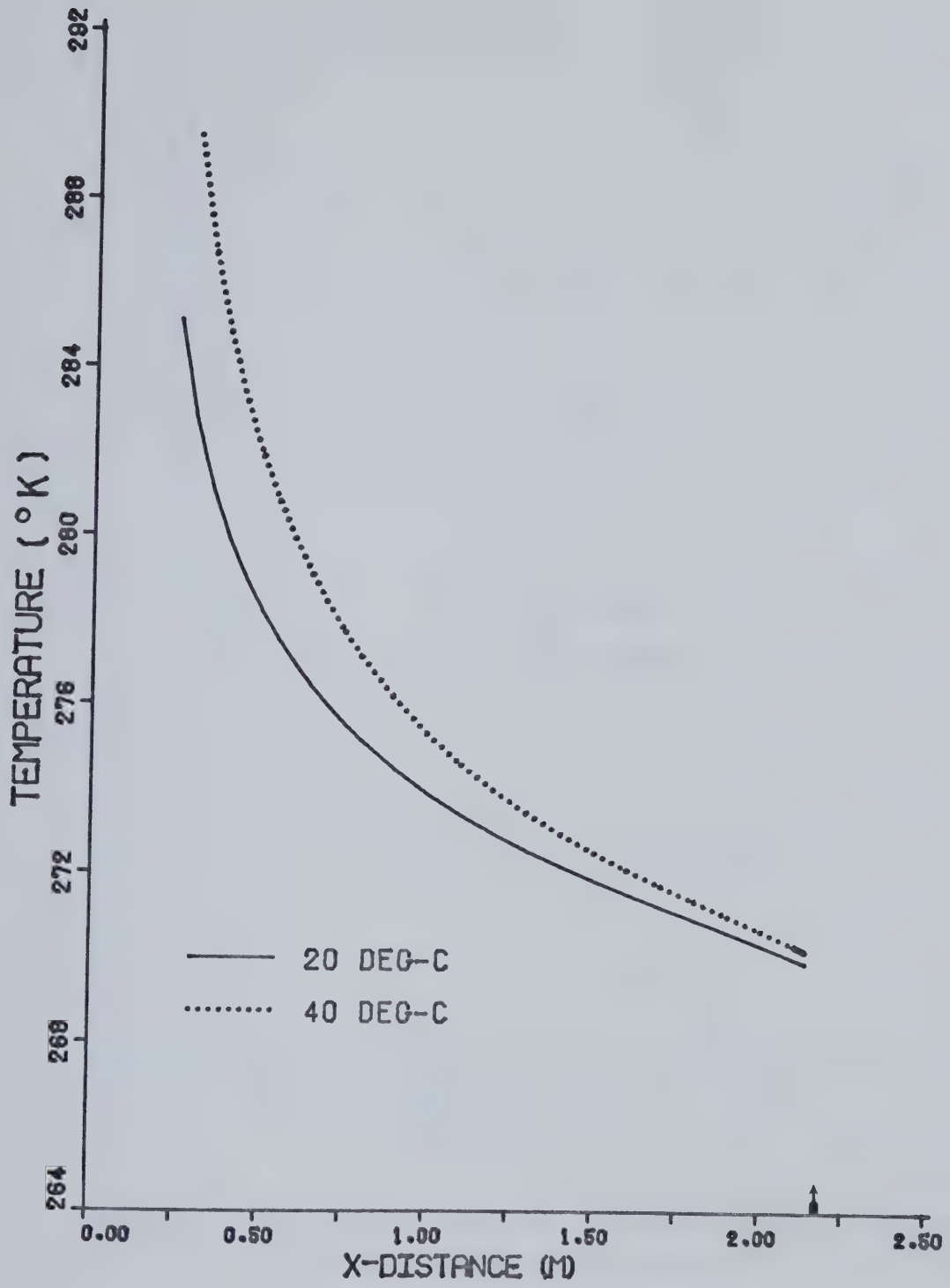

FIGURE 4.5 : The effect of initial spray temperature on the spray temperature as a function of distance from the plenum. The arrow indicates the beginning of the working section.

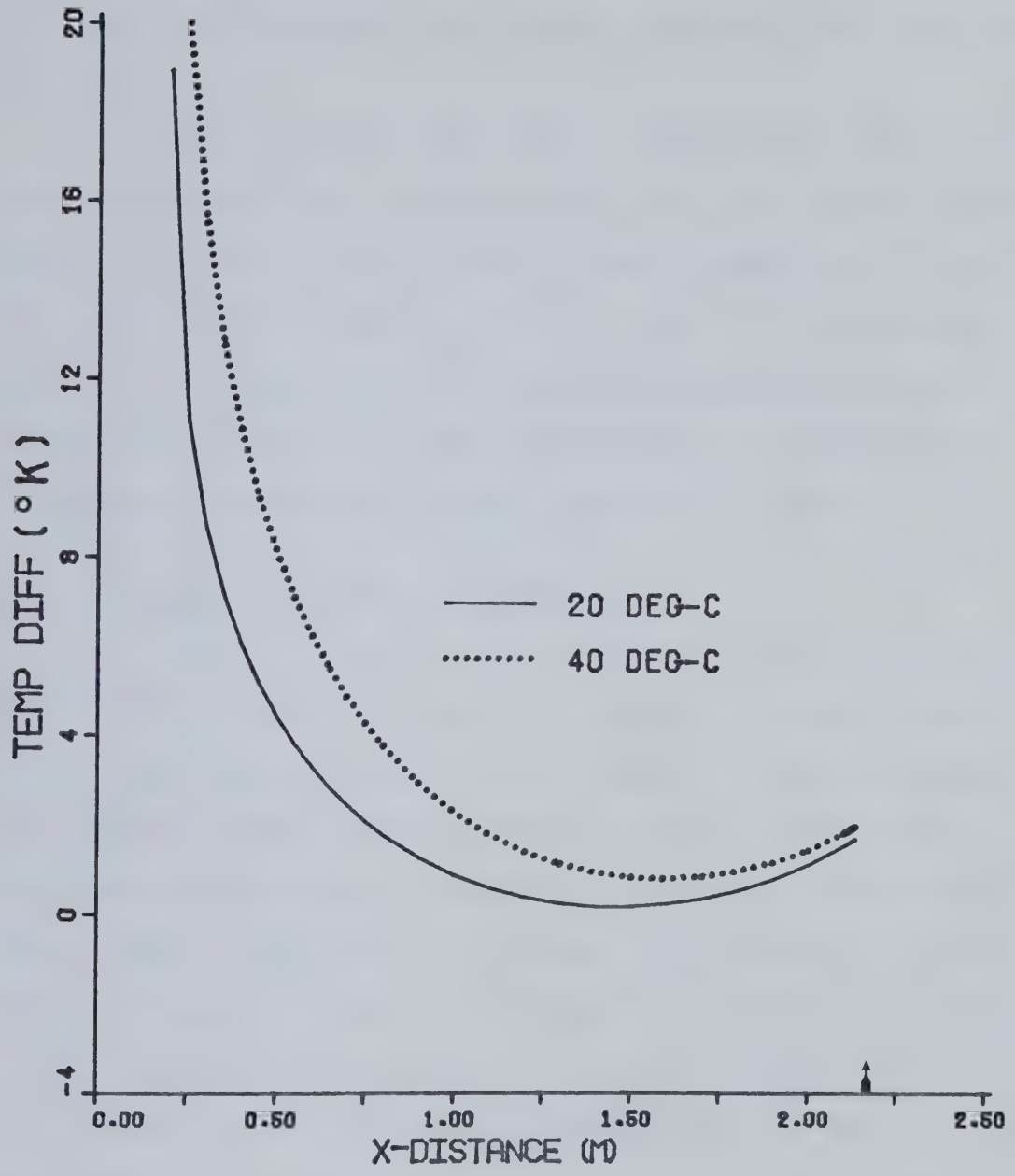

FIGURE 4.6 : The effect of initial spray temperature on the temperature difference (T_c-T) between the spray and the air as a function of distance from the plenum. The arrow indicates the beginning of the working section.

the spray and the air shows only a small dependence on the spray injection temperature.

Since the calculations from the single droplet model give similar results to those from the ensemble model, the earlier conclusion that there is no significant thermal feedback between the spray and the air is supported. An explanation for the result that two droplets of equal size and starting with very different temperatures can end at the working section with very similar temperatures is that the droplet temperature approaches the wet-bulb temperature of the air.

4.5 The Effect of Variation of Droplet Radius

Figures 4.7 and 4.8 show the effect of varying the radius of the droplets. As seen in Figure 4.7, a spray of 10 micron droplets cools faster than a spray of 25 micron droplets. Figure 4.8 shows that the 100 micron radius droplets tend to lag the air temperature by substantial amounts for the entire length of the contraction section. The smallest droplets, having a 10 micron radius, actually cool below the air temperature. Since the calculated relative humidity of the air remains below the saturated value for the entire contraction section (for a plenum relative humidity of 50 percent) and the wet-bulb temperature then remains less than the air temperature, these results suggest that the 10 micron droplet approaches the wet-bulb temperature of the air (and equilibrium) sooner than the larger droplets.

The calculations indicate that the larger droplets lag the air speed by significantly greater amounts than the smaller droplets. The 100 micron droplets, for example, lag the air speed at the working section by 38 m/s while the 10 micron droplets lag the air speed by only

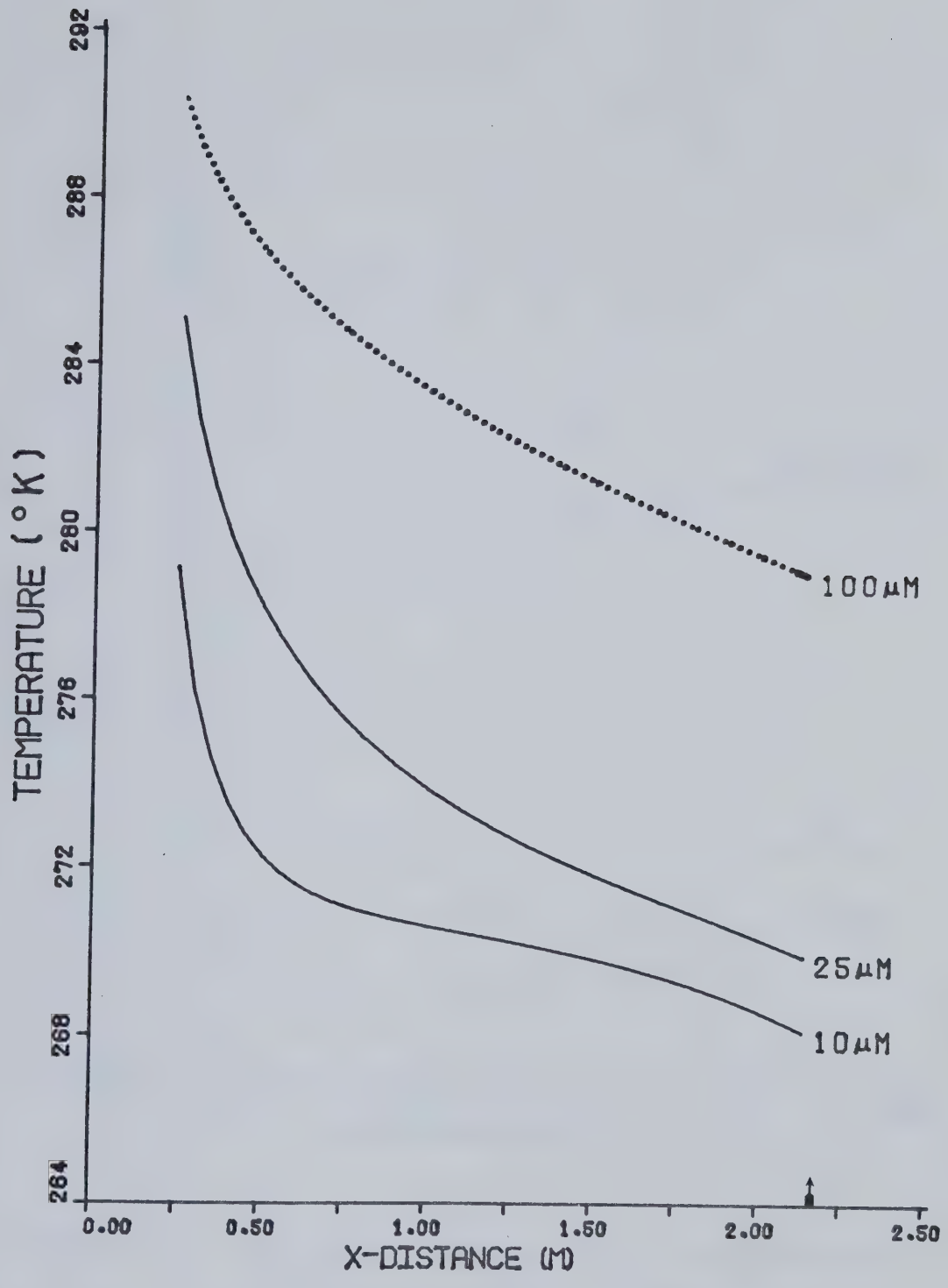

FIGURE 4.7 : The effect of droplet radius on the spray temperature as a function of distance from the plenum. The arrow indicates the beginning of the working section.

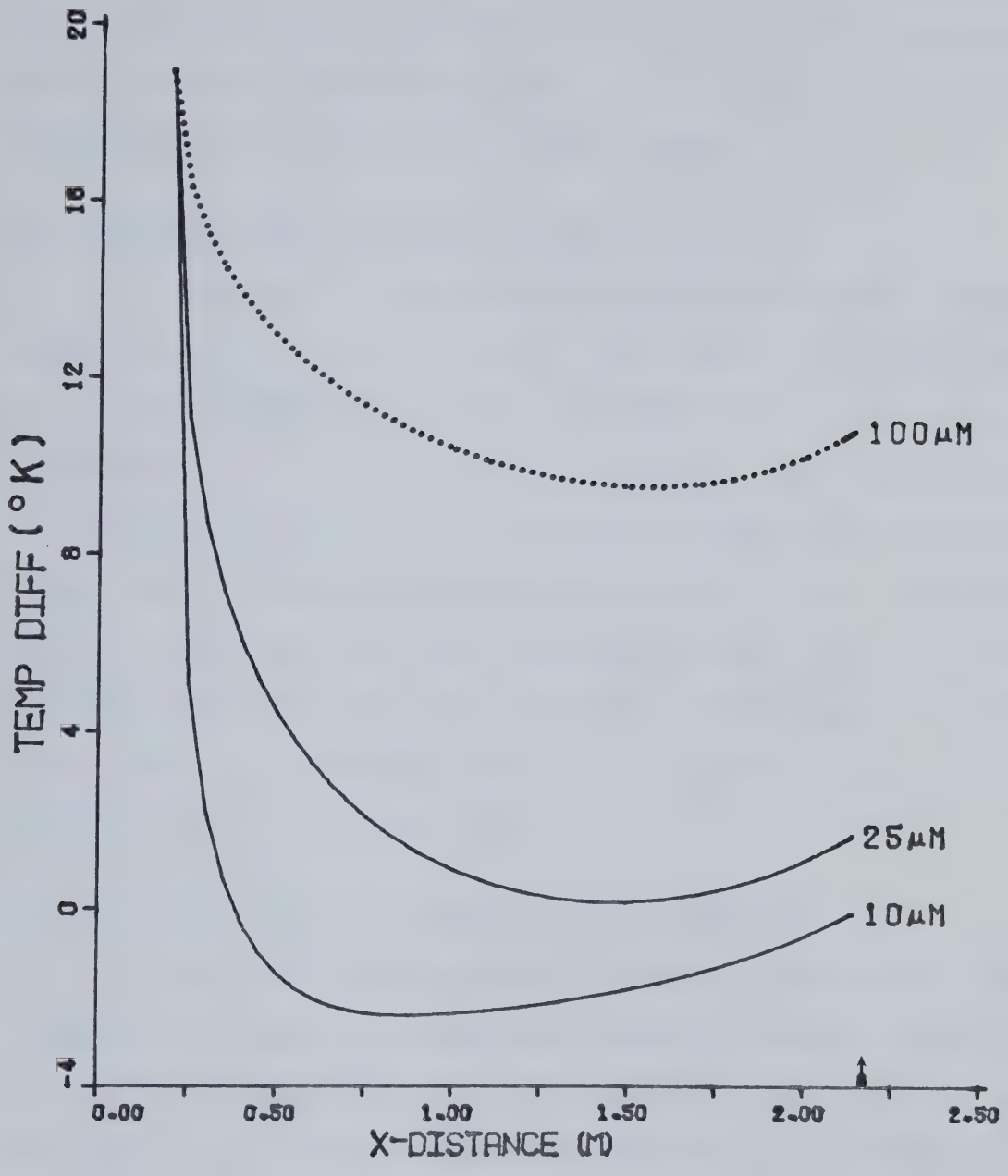

FIGURE 4.8 : The effect of droplet radius on the temperature difference (T_c-T) between the spray and air as a function of distance from the plenum. The arrow indicates the beginning of the working section.

6 m/s. Thus, if it is assumed that the spray reaches the temperature and speed of the air at the working section, as is the case in many icing simulations, significant errors could be incurred.

4.6 The Effect of Variation of the Injection Velocity

The effect of varying the spray injection velocity is shown in Figures 4.9 and 4.10. It is seen that, for these initial conditions, varying the injection velocity has only a small effect on the final spray temperature. It is noted though, that a smaller initial relative velocity between the droplets and the air results in a slower cooling of the spray because heat and mass transfers from the droplets are less initially. Since the injection velocity has a negligible effect on the air temperature, the difference between the spray and air temperatures at the working section has only a small dependence on the injection velocity. This result is indicated by Figure 4.10.

4.7 The Effect of Air Speed on the Droplet Properties

The effect that a variation in the air speed has on the spray temperature and velocity is shown in Figures 4.11 and 4.12. The spray is injected into the air flow at a speed of 3 m/s in all three cases and the slow, medium, and fast tunnel air speeds correspond to plenum speeds of 5, 10, and 20 m/s, respectively. Figure 4.11 indicates that the velocity difference between the spray and the air is greatest for the fast air flow, with the droplets moving at essentially the air speed in the case of the slow air flow.

For the slow and medium air speeds, it is seen in Figure 4.12 that the spray temperature rapidly decreases during the first 0.5 m of the contraction distance and reaches temperatures that are below the air

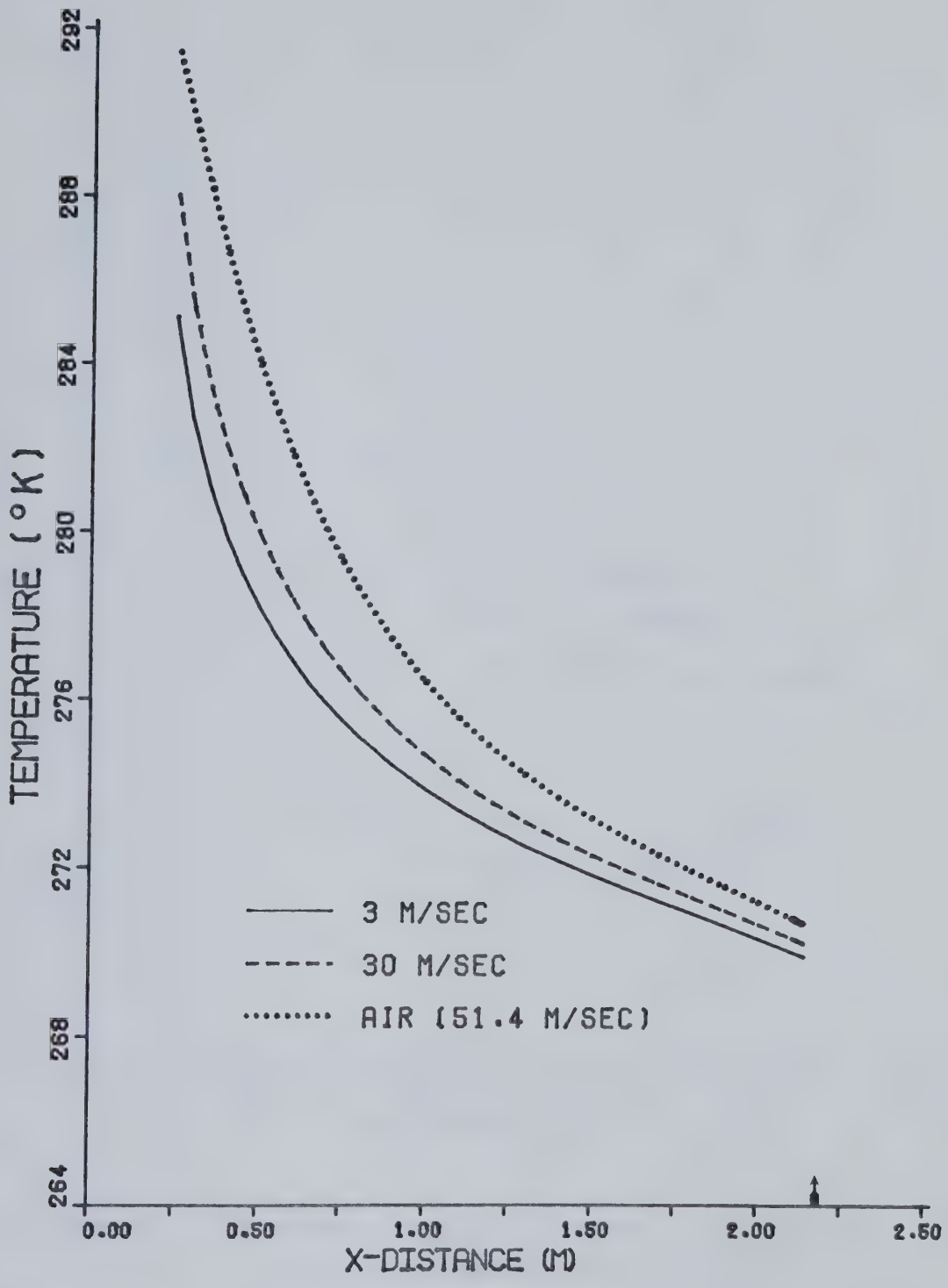

FIGURE 4.9 : The effect of spray injection velocity on the spray temperature as a function of distance from the plenum. The arrow indicates the beginning of the working section.

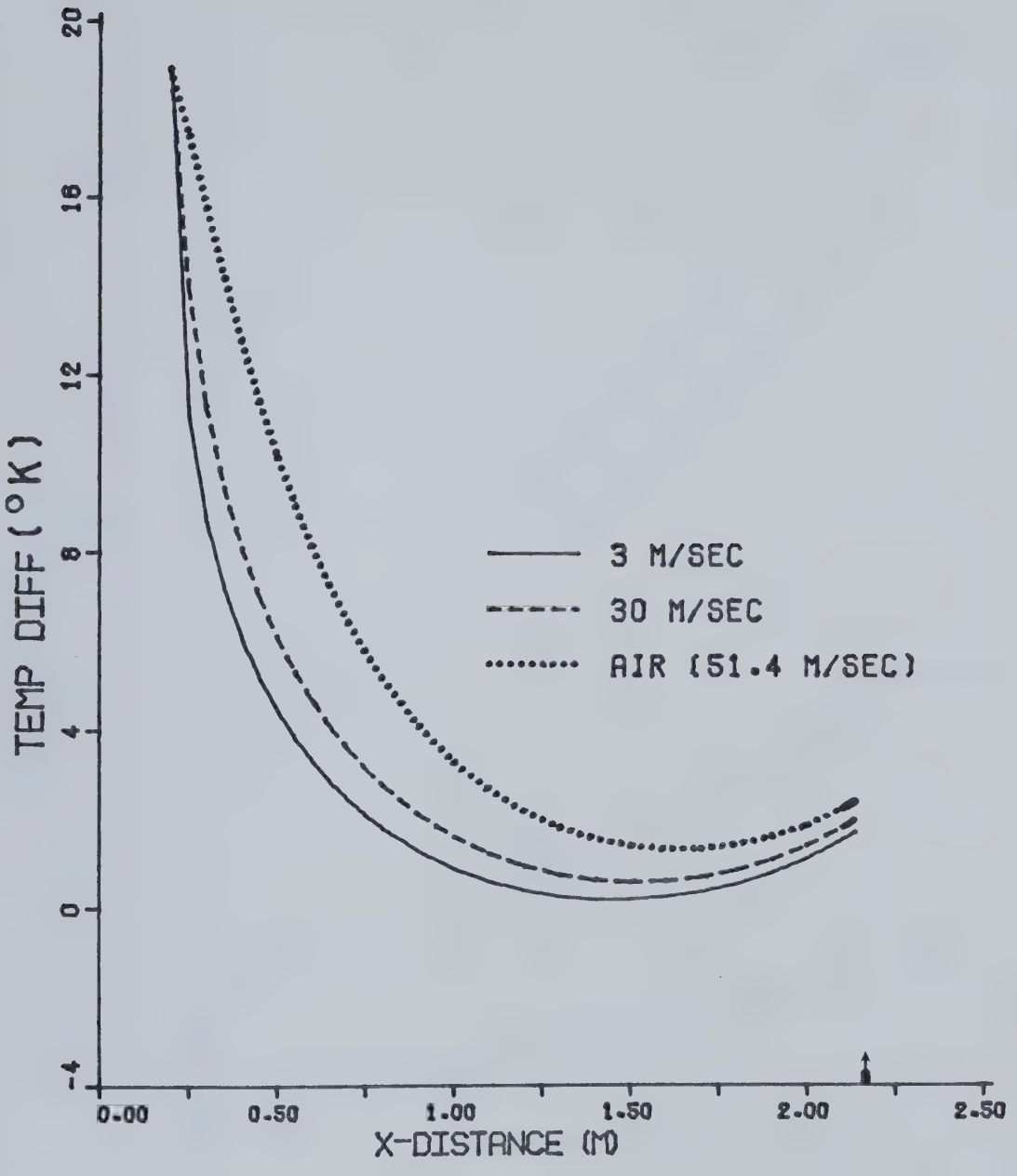

FIGURE 4.10 : The effect of spray injection velocity on the temperature difference (T_c-T) between the spray and air as a function of distance from the plenum. The arrow indicates the beginning of the working section.

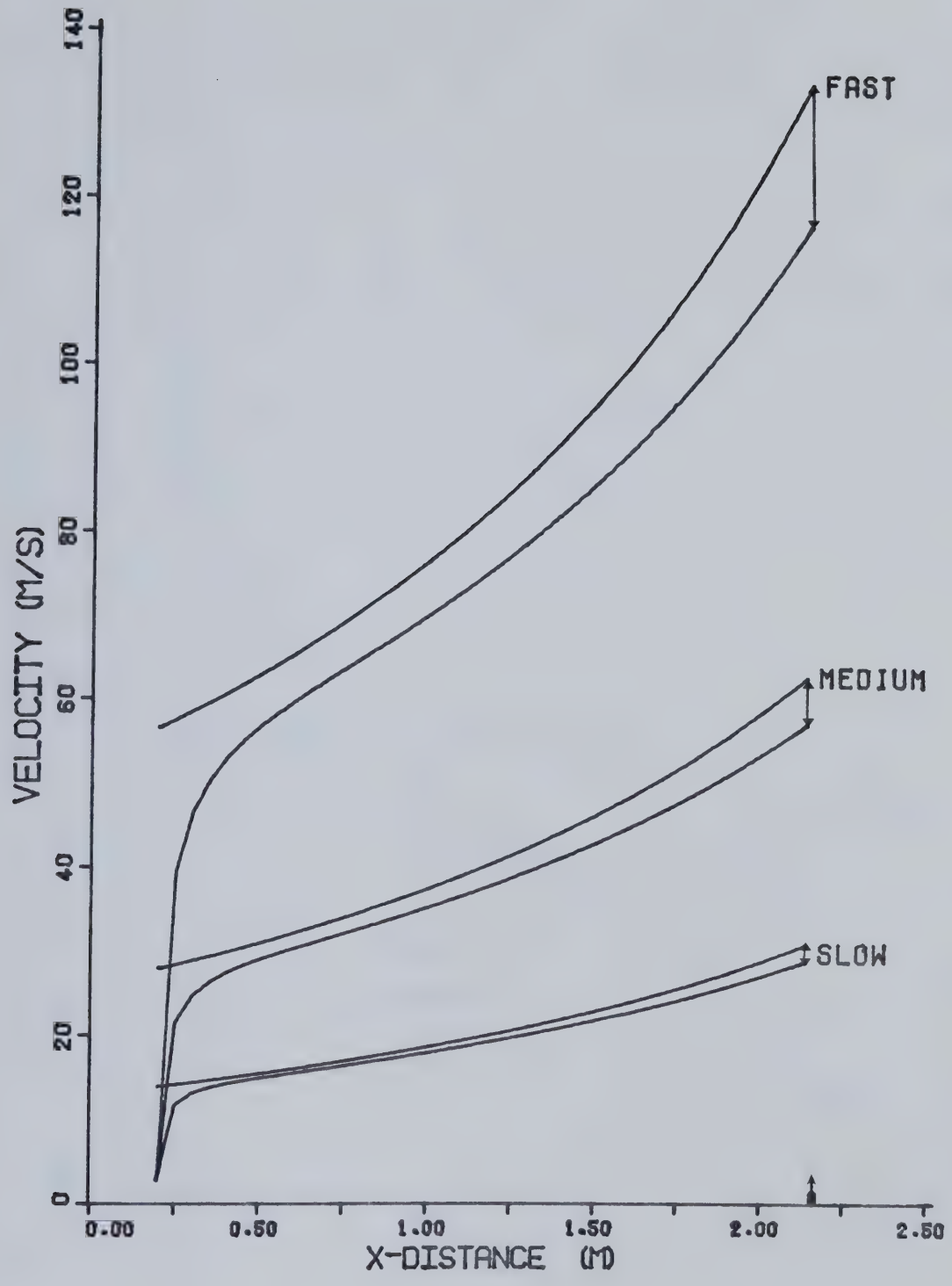

FIGURE 4.11 : The effect of air speed on the one-dimensional spray velocity. The air speed is the upper curve in each case. The slow, medium, and fast air speeds correspond to plenum speeds of 5, 10, and 20 m/s, respectively. The double arrows indicate velocity lags near the working section.

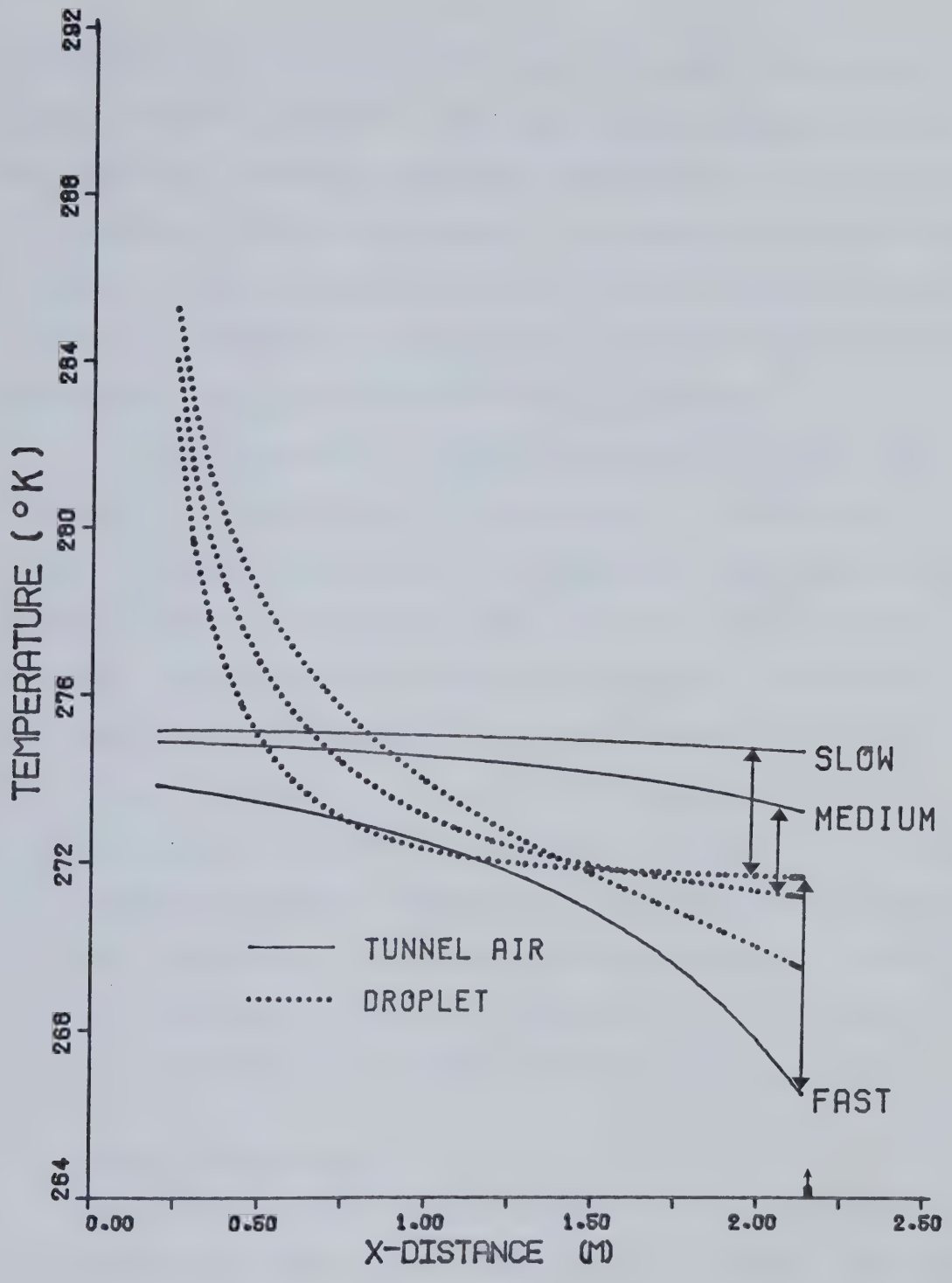

FIGURE 4.12 : The effect of air speed on the air and spray temperature. The air temperature is the solid curve in each case. The slow, medium, and fast air speeds correspond to plenum speeds of 5,10, and 20 m/s, respectively. The double arrows indicate temperature differences near the working section.

temperature. In each of these two cases, the droplet temperature varies slowly during the last half of the tunnel length, thus indicating an approach to the wet-bulb temperature of the air. When the spray is injected into the fast air flow, however, its temperature decreases steadily but is greater than the air temperature for the entire contraction length. In the case of the fast air flow, the spray temperature departs significantly from equilibrium with the air temperature.

When evaluating the effects on the behavior of the spray temperature of a variation in the tunnel speed, it is difficult to isolate the factors that explain the differences. The relations indicated in Figure 5.12 reflect the interaction of a number of factors that determine the state of the air flow and consequently, influence the rate of energy and momentum transfers from a spray droplet. For example, two main factors that compete to determine the changes in the wet-bulb temperature of the air are the increase in the tunnel relative humidity with contraction distance, implying an increase in the wet-bulb temperature, and the decrease in air temperature with contraction distance, implying a decrease in the wet-bulb temperature. The net effect of these two factors can have a large influence on the droplet temperature.

4.8 Summary of the Results

The following conclusions are drawn by this parametic study. The temperatures of the spray and moist air at the working section are practically independent of the initial spray temperature. The effect of varying the liquid water content of the spray is small. The reason for these results is that the spray and vapor fluxes are only a small fraction of the total mass flow. Thus, there is no significant thermal feedback

between the spray and the air. The droplet temperature is largely controlled by properties of the surrounding air and tends to approach the wet-bulb temperature of the air. It is found that a substantial control over the thermal state of the spray at the working section is possible through control of the plenum relative humidity. A large initial relative velocity between the injected spray and the air helps to promote a more rapid approach of the spray to thermal equilibrium with the air. In addition, droplets having a radius of say, 10 microns, approach the wet-bulb temperature of the air at a much faster rate than larger droplets having a radius of 100 microns. Thus, a shorter duct length can be used for the smaller droplets to achieve an effective equilibrium with the air. Finally, for plenum air speeds of 20 m/s, the temperature and the velocity of the spray significantly lag that of the air. For plenum air speeds of 5 and 10 m/s, the spray approaches the velocity and wet-bulb temperature of the air, while it remains substantially out of equilibrium with the air in the case where the plenum air speed is 20 m/s.

CHAPTER 5

CONCLUSIONS AND RECOMMENDATIONS

5.1 Final Conclusions

The present study has developed a model of general applicability for determining the actual spray and air dynamics and thermodynamics in any testing facility. MKS units were used for all variables and constants. The properties of the spray and air, averaged over a cross-sectional area perpendicular to the tunnel axis, were determined using a one-dimensional numerical model of the flow. The main properties calculated were the temperatures and velocities of the spray and air, the droplet size, and the air pressure. The single droplet model and the ensemble model were developed for this purpose and the governing equations were programmed in FORTRAN IV language for solution on a digital computer. The single droplet model, introduced in Chapter 3, applies to situations where the spray has only a negligible influence on the air flow. The ensemble model, discussed in Chapter 3, is a modified version of the simpler single droplet model, applicable to cases where the contributions of the spray to the moist air flow have to be considered.

A limited parametric study was performed to determine the effects of the initial moist air and water spray conditions on the state of the flow at the working section of the NRC high speed icing tunnel. A number of significant results were obtained from this study. It was found that the final solutions given by the two models were essentially identical for the liquid water contents typical of an icing situation. It was concluded that there was no significant thermal feedback between the spray and the moist air. The spray temperature at the working section

of the tunnel was found to be sensitive to the relative humidity of the air. It was considered that, for sufficient duct length, the droplets tended to approach the wet-bulb temperature of the air, with 10 micron droplets approaching this temperature more quickly than the 100 micron droplets. For plenum air speeds of 5 and 10 m/s, it was found that the velocity of the 25 micron droplets tended to approach the velocity of the air and the droplet temperature tended to approach the wet-bulb temperature before reaching the working section. When the plenum speed was 20 m/s, comparison with the results for the slower tunnel speeds indicated that the droplet properties remained significantly out of equilibrium with the air properties for the entire contraction section.

5.2 Final Recommendations

The following recommendations are given, some of which have been mentioned in previous discussions:

1. Droplet freeze-out processes should be incorporated into the droplet growth and thermodynamic equations. In this respect, the inclusion of particulate matter with the moist air flow would contribute to simulation of freeze-out processes and could ensure that more realistic tunnel supersaturations result when the plenum relative humidity is near saturation.
2. Calculations performed for flow of a single droplet in the NRC high speed icing tunnel indicate that the history term should be included in the droplet momentum equation when the injection velocity of the droplet relative to the air is small. This result was obtained using the droplet accelerations that were calculated by omitting the history term from the equations of motion.

3. Consideration should be given to relaxing the assumption that the vapor introduced by evaporation of the spray is immediately mixed with the ambient moist air. It is suggested that an entropy flux equation might be derived that accounted for two vapor temperatures -- one temperature associated with "recent" changes in the vapor density introduced by evaporation and condensation of the spray and one associated with the well-mixed portion of the moist air.
4. The present ensemble model should be expanded to incorporate a non-uniform size distribution.

Abraham, F. F., 1968: A physical interpretation of the structure of the ventilation coefficient of freely falling water drops. J. Atmos. Sci., 25, 76-81

Baldwin, R., 1975: A theoretical model for cave air flow: The chimney effect. M. Sc. Thesis, Dept. of Geography, Univ. of Alberta, 134 pp.

Beard, K. V. and H. R. Pruppacher, 1971: A wind tunnel investigation of the rate of evaporation of small water drops falling at terminal velocity in air. J. Atmos. Sci., 28, 1455-1464.

Beard, K. V. and H. R. Pruppacher, 1969: A determination of the terminal velocity and drag of small water drops by means of a wind tunnel. J. Atmos. Sci., 26, 1066-1072.

Bird, R. B., W. E. Stewart, and E. N. Lightfoot, 1960. Transport Phenomena. New York, Wiley, 780 pp.

Borovikov, M. I., I. I. Gaivoronskii, E. G. Kostarev, I. P. Mazin, E. G, Zak, V. V. Kostarev, I. P. Mazin, V. E. Minervin, A. Kh. KhRgian, 1963: Cloud Physics . A. KhKhrgian, Ed., Jerusalem, Israel Program for Scientific Translations, 392 pp.

Crowe, C. T., 1978: On the vapor-droplet flows including boundary-droplet effects. Proc. of the Two-Phase Flow and Heat Transfer Symposium-Workshop, Fort Lauderdale, 385-405.

Filippov, G. A., 1970: Determination of the degree of inequilibrium of the expansion of two-phase media. Heat Transfer-Soviet Research, 2, 146-150. (Trans. by Scripta Technica Inc., Wash., D.C.)

Fitzgerald, J. W., 1972: A study of the initial phase of cloud droplet growth by Condensation: Comparison between theory and observation. Ph. D. Thesis, Dept. of Geophys. Sci., Univ. of Chicago, 138 pp.

Fuchs, N. A., 1959: Evaporation and Droplet Growth in Gaseous Media. New York, Pergamon Press, 72 pp.

Fukuta, N. and L. A. Walter, 1970: Kinetics of hydrometeor growth from a vapor-spherical model. J. Atmos. Sci., 27, 1160-1172.

Iribarne, J. V. and W. L. Godson, 1973: Atmospheric Thermodynamics. Dordrecht, Holland, D. Reidel Publ. Co., 213 pp.

Joe, P. I., 1975: Investigation of the bouncing of supercooled water droplets from an artificially growing hailstone. M. Sc. Thesis, Dept. of Physics, Univ. of Toronto, 254 pp.

Katchalsky, A. and P. F. Curran, 1967: Nonequilibrium Thermodynamics in Biophysics. Cambridge, Mass., Harvard Univ. Press, 244 pp.

Kalinin, A. V., 1970: Derivation of fluid mechanics equations for a two-phase medium with phase changes. Heat Transfer-Soviet Research, 2, 83-96. (Trans. by Scripta Technica Inc., Wash.,D.C.)

Kern, D. Q., 1950: Process Heat Transfer. New York, McGraw Book Co., 66-74.

Landau, L. D. and E. M. Lifshitz, 1959: Fluid Mechanics. London, Pergamon Press, 529 pp.

LeClair, B. P., A. E. Hamielec, and H. R. Pruppacher, 1970: A numerical study of the drag on a sphere at low and intermediate Reynolds numbers. J. Atmos. Sci., 27, 308-315.

List, R. J., 1951: Smithsonian Meteorological Tables, Sixth Revised Edition. Washington, D.C., Smithsonian Institution, 527 pp.

Lowe, P. R., 1977: An approximating polynomial for the computation of saturated vapor pressure. J. Appl. Meteor., 16, 100-103.

Lozowski, E. P., J. R. Stallabrass, and P. F. Hearty, 1979: The Icing of an Unheated Non-Rotating Cylinder in Liquid Water Droplet - Ice Crystal Clouds. NRC Laboratory Report LTR-LT-96.

Mason, B. J., 1957: The Physics of Clouds, first edition. Oxford, Claredon Press.

Meteorological Office, 1960: Handbook of Aviation Meteorology. London, Her Majesty's Stationary Office, 398 pp.

Neiburger , M. and C. W. Chien, 1960: Computation of the growth of cloud drops by condensation using an electronic digital computer. Physics of Precipitation, Geophys. Monogr. No. 5, Washington, D.C., American Geophys. Union, 191-210.

Pearcey, T. and G. W. Hill, 1956: The accelerated motion of droplets and bubbles. Aust. J. of Physics, 9, 19-30.

Pruppacher, H. R. and J. D. Klett, 1978: Microphysics of Clouds and Precipitation. Dordrecht, Holland, D. Reidel Publishing Company, 656 pp.

Rogers, R. R., 1976: A Short Course in Cloud Physics. London , Pergamon Press, 217 pp.

Sartor, J. D. and C. E. Abbott, 1975: Prediction and measurement of the accelerated motion of water drops in air. J. Appl. Meteor., 14, 232-239.

Shapiro, A. H., 1953: The Dynamics and Thermodynamics of Compressible Fluid Flow, Vol. 1. New York, The Ronald Press Co., 633 pp.

Shapiro, A. H., 1961: Shape and Flow. Garden City, New York, Anchor Books, 171 pp.

Solbrig, C. E. and D. Gidaspow, 1976: Equilibrium homogeneous transient two-phase flow. Proc. of the NATO Study Institute, Istanbul, Turkey, 1171-1200.

Vath, K. A., 1978: Meteorological icing conditions. Icing Testing for Aircraft Engines, AGARD Conf. Proc. No. 236, London.

Watts, R. E., 1971: Relaxation time and steady evaporation rate of freely falling raindrops. J. Atmos. Sci., 28, 219-225.

Willbanks, C. E. and R. J. Shultz, 1973: Analytical Study of Icing Simulation For Turbine Engines in Altitude Test Cells , AEDC-TR-73-144. Tullahuma, Tennessee, Arnold Engineering Development Center.

Woo, S. E. and A. E. Hamielec, 1971: A numerical method for determining the rate of evaporation of small water drops falling at terminal velocity in air. J. Atmos. Sci., 28, 1448-1454.

APPENDIX A

LIST OF SYMBOLS

A	flow cross-sectional area
c_{pd}, c_{pv}	specific heat capacities at constant pressure for dry air and water vapor, respectively
c_{vd}, c_{vv}	specific heat capacity at constant volume for dry air and water vapor, respectively
c_w	specific heat capacity for water
E	emissivity of water
e	partial vapor pressure of moist air
e_c	saturation vapor pressure over a droplet
e_{sat}	saturation vapor pressure with respect to plane water surface
F_S	entropy flux crossing a cross-sectional area
$\overline{f}$	mean ventilation coefficient
g	acceleration of gravity
k	thermal conductivity of moist air
ℓ_v	specific latent heat of evaporation
m	mass
m_c	mass of a droplet
m_T	mass of system
M	Mach number
N	number of droplets per unit volume
$\overline{Nu}$	mean Nusselt number
Pr	Prandtl number

P	pressure of moist air
Q_d, Q_w	mass flux of dry air and water substance, respectively
q	specific humidity
R_d, R_v	specific gas constants for dry air and water vapor, respectively
Re	Reynolds number
RH	relative humidity
r	mixing ratio
r_c	droplet radius
S_T	entropy of spray and moist air system
Sc	Schmidt number
$\overline{Sh}$	mean Sherwood number
s_d, s_v, s_c	specific entropy of dry air, vapor, and spray, respectively
T (or T_d)	temperature of moist (and dry) air
T'	virtual temperature
t	time
U	one-dimensional velocity (moist air)
U_c	one-dimensional spray velocity
x	axial distance from plenum
ω	mass flux of air injected by a sprayer nozzle
μ	dynamic viscosity of air
ν	kinematic viscosity of air
ρ	mass density
ρ_w	density of water
γ	ratio of specific heat capacities for moist air = c_p/c_v
σ	Stefan-Boltzmann constant
σ'_{WA}	surface tension of water in air

APPENDIX B

MACH NUMBER FORMULATION FOR FRICTIONLESS, ADIABATIC FLOW

The equations that determine the adiabatic frictionless one-dimensional flow of dry air through the contraction of the wind tunnel can be rewritten in terms of the local Mach number. This non-dimensional variable is defined as the ratio of the local flow speed to the speed of sound. For adiabatic flow of dry air treated as a perfect gas, the Mach number is given from Equation 2.2.8 as, $M = U/(\gamma R_d T)^{1/2}$.

The Bernoulli equation for compressible adiabatic flow can be integrated to yield Equation 2.2.5,

$$\frac{U_2^2}{2} + \frac{\gamma}{\gamma - 1}\frac{P_2}{\rho_2} = \frac{U_1^2}{2} + \frac{\gamma}{\gamma - 1}\frac{P_1}{\rho_1}$$

Using the Perfect Gas Law, and the definition of Mach number in the form, $U^2 = M^2 \gamma R_d T$, Equation 2.2.5 can then be written in terms of the temperature and Mach number as,

$$\frac{\gamma R_d T_2 M_2^2}{2} + \frac{\gamma R_d T_2}{\gamma - 1} = \frac{\gamma R_d T_1 M_1^2}{2} + \frac{\gamma R_d}{\gamma - 1} T_1 \qquad (B.1)$$

It is assumed that γ is a constant in the above expression. Equation B.1 may be rearranged to give the relation,

$$T_2 \left(M_2^2 + \frac{2}{\gamma - 1} \right) = T_1 \left(M_1^2 + \frac{2}{\gamma - 1} \right) \qquad (B.2)$$

Substitution of the Perfect Gas Law and the definition of the Mach number into the continuity equation, (2.2.4), results in an expression relating the temperature to the air density for two points along the flow direction. The expression is,

$$\rho_2 = \frac{\rho_1 A_1 M_1 T_1^{\frac{1}{2}}}{A_2 M_2 T_2^{\frac{1}{2}}} \qquad (B.3)$$

Equation 2.2.3 (Poisson's equation), describing an adiabatic expansion or compression of a perfect gas, can be written in terms of density and temperature by applying the Perfect Gas Law. The result is,

$$T_2 = \left(\frac{T_1}{\rho_1^{(\gamma-1)}} \right) \rho_2^{(\gamma-1)} \qquad (B.4)$$

Combining Equations B.2, B.3, and B.4, a relation is obtained that links the Mach number to the ratio of the cross-sectional areas at positions x_1 and x_2. Using $\gamma = 7/5 = 1.4$, the relation is written as,

$$\frac{M_1}{M_2} \left(\frac{M_1^2 + 5}{M_2^2 + 5} \right)^3 = \frac{A_2}{A_1} \qquad (B.5)$$

APPENDIX C

CALCULATION OF THE SPRAYER AIR FLUX FOR THE NRC TUNNEL

The object of the following discussion is to show that the mass flux of the air that is injected through the nozzles is small compared to the mass flux without the sprayers.

The air that is injected with the spray is contained within the spray nozzle between an outer tube having a diameter of 3.1 mm and an inner tube having a diameter of 1.3 mm. The water that is injected is contained within this inner tube and a smaller concentric (hollow) tube having a radius of 0.51 mm.

The assumptions that are used to obtain an estimate of this flux include the following:

1. The air is flowing at the sonic speed through the nozzle (that is, the nozzle is a critical nozzle).
2. The air is heated to 30°C within the nozzle.
3. Upon injection, the air expands adiabatically to achieve a tempera- of -40°C and a pressure equal to the (controlled) ambient tunnel pressure (Lozowski, personal communication).

A relation may be obtained connecting the mass flux to the temperature and pressure of the injected air. The expression for the mass flux is written as,

$$\omega = (\rho A c)_{nozzle} \qquad (C.1)$$

where c is the sonic speed. The speed of sound for a perfect gas is determined from the air temperature and is given by, $c^2 = \gamma RT$. Substituting this expression into the mass flux evaluation, the result is,

$$\omega_n = P_n A_n \sqrt{\frac{\gamma}{R_d T_n}} \qquad (C.2)$$

where the subscript n describes variables within the nozzle. The air pressure within the nozzle is calculated using the adiabatic expansion relation (Poisson's equation),

$$\frac{P_i}{P_n} = \left(\frac{T_i}{T_n}\right)^{c_p/R_d} \qquad (C.3)$$

where the subscript i describes variables after injection. The injected air flux is determined using Equations C.2 and C.3.

For the initial conditions given in Section 4.1, the calculated tunnel pressure at the sprayers (P_i) is 99,710 Pascals. The pressure within the sprayer nozzle, given by Equation C.3, is approximately 250,130 Pascals. Using T_n = 30°C and $A_n = 6\text{x}10^{-6}\text{m}^2$, the injected mass flux is obtained from Equation C.2 and is $6\text{x}10^{-3}$kg/s. The results from calculations for flow in the NRC tunnel,on the other hand, give a tunnel air flux at the sprayers of 13.4 kg/s. The ratio of the injected flux to the tunnel air flux, $4.5\text{x}10^{-4}$, indicates that the injected flux may be neglected relative to the air flux that would result without the nozzles.

APPENDIX D

EQUILIBRIUM ENTROPY FLUX

According to the Second Law of Thermodynamics, the specific entropy of a system in equilibrium is a well-defined function of its state. Given a system in equilibrium consisting of m_d kilograms of dry air, m_c kilograms of condensed water in the form of droplets and m_v kilograms of the saturated vapor, the specific entropy of each of the above components is a function of two independent thermodynamic (or state) variables. Accordingly, expressions can then be written for the contribution of each component to the total entropy. Letting S_T denote the total entropy of this system, letting S_d, S_v, and S_c denote the entropy of the dry air, vapor and droplets, respectively, and letting s_d, s_v, and s_c denote the corresponding specific entropy quantities, the total entropy of the system is given by,

$$S_T = m_d s_d + m_v s_v + m_c s_c \tag{D.1}$$

For an equilibrium (reversible) change in this state, the change in the total entropy is written,

$$DS_T = DS_d + DS_v + DS_c$$

where D refers to the total differential. For each component,

$$\begin{aligned} DS_d &= m_d Ds_d \\ DS_v &= m_v Ds_v + s_v Dm_v \\ DS_c &= m_c Ds_c + s_c Dm_c \end{aligned} \tag{D.2}$$

where $Dm_v = -Dm_c$. If pressure and temperature are the state variables used, it is said that an equilibrium expansion or contraction of the system occurs if the temperatures of all three components are equal to each other and if the vapor pressure of the air is maintained at the equilibrium value for the droplets. In order to simplify the derivations, the equilibrium vapor pressure for the droplets is approximated by the saturation vapor pressure with respect to a plane water surface. Calculations for a 10 micron droplet at a temperature of 20°C, for example, indicate that the factor by which curvature increases the equilibrium vapor pressure above the saturation vapor pressure is 1.000086.

According to Iribarne and Godson (1973, p. 75), total differential expressions are given for the change in the specific entropy of each component if changes in the variables occur under equilibrium processes. The relations are,

$$Ds_d = \left[\frac{\partial s_d}{\partial P}\right]_{T,m_T} dT + \left[\frac{\partial s_d}{\partial T}\right]_{P,m_T} dP = c_{pd} D(\ell n\, T) - R_d D(\ell n\, P_d)$$

$$Ds_v = \left[\frac{\partial s_v}{\partial P}\right]_{T,m_T} dT + \left[\frac{\partial s_v}{\partial T}\right]_{P,m_T} dP = c_{pv} D(\ell n\, T) - R_v D(\ell n\, P_d)$$

$$Ds_c = \left[\frac{\partial s_c}{\partial T}\right]_{P,m_T} dT = c_w D(\ell n\, T) \qquad (D.3)$$

where $\left(\frac{\partial s}{\partial P}c\right)_{T,m} \simeq 0$.

The subscript m_T is used to describe partial differentiation with the mass composition of the system held constant.

It can be shown that the specific heat quantities, c_{pd} and c_{pv}, remain constant if the gas behaves according to the Perfect Gas Law (Shapiro, 1953, p. 42). If it is also assumed that the specific heat of

water remains constant for the small change, $D(\ell nT)$, Equations D.3 are easily integrated to obtain the specific entropy of each component. The result is,

$$s_d = s_{d_0} + c_{pd}\ell n\frac{T}{T_0} - R_d\ell n\frac{P_d}{P_{d_0}}$$

$$s_v = s_{v_0} + c_{pv}\ell n\frac{T}{T_0} - R_v\ell n\frac{e_{sat}(T)}{e_{sat}(T_0)}$$

$$s_c = s_{c_0} + c_w\ell n\frac{T}{T_0} \qquad (D.4)$$

The subscript 0 denotes a quantity measured (or calculated) at some reference equilibrium state.

Using Equations D.3, it can be shown that changes in the total entropy of the moist air and spray system that is in equilibrium depend only on changes in the state variables, T and P_d, and in changes of composition. In other words, changes in the total entropy are independent of the reference state chosen.

It is useful to introduce two additional relations, the Clausius-Clapeyron Equation (Iribarne and Godson, 1973, p. 62),

$$\frac{D\ (\ell n\ e_{sat})}{D\ T} = \frac{\ell_v(T)}{R_v\ T^2} \qquad (D.5)$$

and Kirchhoff's Law (Ibid, p. 76),

$$D\ \ell_v = (c_{pv} - c_w)dT \qquad (D.6)$$

The quantity, ℓ_v, in the above relations refers to the specific latent heat of vaporization. Using Equation D.6, the Clausius-Clapeyron

equation is integrated by parts to yield an expression for the saturation vapor pressure. The result of the integration is

$$R_v \ell n \frac{e_{sat}(T)}{e_{sat}(T_0)} = - \int_{T_0}^{T} \frac{D}{DT}\left(\frac{\ell_v}{T} \right) DT + \int_{T_0}^{T} \frac{1}{T} \frac{D}{DT}(\ell_v)\, DT$$

$$= \frac{\ell_v(T_0)}{T_0} - \frac{\ell_v(T)}{T} + (c_{pv} - c_w) \ell n \frac{T}{T_0} \qquad (D.7)$$

From Kirchhoff's Law in integrated form,

$$\ell_v = (c_{pv} - c_w)(T - T_0) + \ell_{v_0}$$

and Equation D.7, it can be shown that,

$$s_v(T) - s_c(T) = \frac{\ell_v(T)}{T} \qquad (D.8)$$

If the following mass conservations relations,

$$m_{w_0} = \text{constant} = m_v + m_c$$
$$m_{d_0} = \text{constant} = m_d$$

are substituted into Equation D.1, it follows that,

$$S_T = m_d s_d + m_v (s_v - s_c) + m_{w_0} s_c \qquad (D.9)$$

Using the appropriate specific entropy relations (Equations D.4) and substituting Equation D.8 into (D.9), the result is,

$$S_T = m_d\, s_{d_0} - c_{pd} \ell n\, T_0 + R_d \ell n\, P_{d_0} - m_{w_0} c_w \ell n\, T_0$$
$$+ m_w c_w \ell n\, T + m_d\, c_{pd} \ell n\, T - R_d \ell n\, P_d + \frac{m_v \ell_v(T)}{T} \qquad (D.10)$$

The constant terms on the right hand side may be combined to give the reference entropy, S_0. The following relation results:

$$S = S_0 + (c_{pd}m_d + c_w m_{w_0}) \ln T + \frac{m_v \ell_v(T)}{T} - m_d R_d \ln P_d \qquad (D.11)$$

Equation D.11 states that the total entropy depends only on the state of the system and on the composition of the droplet and moist air system.

APPENDIX E

DERIVATION OF AN ENTROPY FLUX EQUATION

Let us consider the case where the water droplets and the moist air are moving in a tunnel of varying cross-sectional area. The droplets and the moist air are each characterized by different temperatures and axial velocities so that a nonequilibrium flow is described. In addition, we assume that the partial vapor pressure at any cross-section may depart from its equilibrium value.

The rate of accumulation of total entropy within a control volume may be determined by applying the Reynolds Transport Theorem to the entropy flow. The result is

$$\frac{DS_T}{Dt} = \frac{\partial}{\partial t} \int_{\upsilon} \Sigma \rho_i s_i \, d\upsilon + \int_{S} \Sigma \rho_i s_i \vec{U}_i \cdot d\vec{A} \qquad (E.1)$$

The summation accounts for contributions from the dry air, water vapor, and droplets. Since steady-state conditions are assumed, the entropy does not accumulate because of internal sources within the control volume. Since it is also assumed that the control volume is adiabatically insulated at the lateral surface, entropy can not be exchanged at this surface (also, the flow is one-dimensional). For steady-state flow in the tunnel, the total entropy in the control volume remains constant only if no net flux of entropy crosses through the cross-sectional flow areas. If it is assumed that the total entropy within the control volume is constant, an entropy equation can be derived to describe the coupled state of the system.

Referring to the control volume in Figure 3.1, the total entropy flux that crosses the area, A = A(x), is constant and is written,

$$F_{S_0} = \text{constant} = F_S(x) = F(x+dx) \qquad (E.2)$$

where the variable F_S refers to an entropy flux and F_{S_0} is its conserved value. Using the appropriate one-dimensional velocities, the entropy flux crossing the area, A, is given by,

$$F_S(x) = (s_d\rho_d U + s_v\rho_v U + s_c\rho_c U_c)A \Big|_x \qquad (E.3)$$

The specific entropy variables, s_d, s_v, and s_c are defined in Appendix D. If the mass continuity equations,

$$\begin{aligned} \rho_d UA &= Q_d = \text{constant} \\ (\rho_v U + \rho_c U_c)A &= Q_w = \text{constant} \end{aligned} \qquad (E.4)$$

are substituted into (E.3), the entropy flux at any position x is given by,

$$F_S(x) = s_d Q_d + \rho_v UA \left[s_v(T) - s_c(T_c)\right] + s_c Q_w \qquad (E.5)$$

The specific entropy variables are, of course, evaluated at the appropriate temperatures.

Let us define an equilibrium reference state in which the temperatures of the droplets and the moist air are equal. We consider that the reference temperature, T_0, is equal to the saturation temperature where, for practical purposes, saturation is defined with respect to a plane water surface. The specific entropy quantities at the reference state are denoted as s_{d_0}, s_{v_0}, and s_{c_0}. Using the appropriate specific entropy quantities given in Appendix D, the entropy flux crossing a cross-sectional area is written,

$$F_S(x) = \left(Q_d s_d(T_0) + Q_w s_c(T_0)\right) + Q_d\left(c_{pd}\ell n \frac{T}{T_0} - R_d \ell n \frac{P_d}{P_{d_0}}\right)$$

$$+ Q_w c_w \ell n \frac{T_c}{T_0} + \rho_v UA\left(s_v(T) - s_c(T_c)\right) \qquad (E.6)$$

The entropy difference, $s_v(T) - s_c(T_c)$, for nonequilibrium temperatures, T and T_c, and for the nonequilibrium vapor pressure, e, is given by,

$$s_v(T) - s_c(T_c) = \left(s_v(T_0) - s_c(T_0)\right) + c_{pv}\ell n \frac{T}{T_0} - R_v \ell n \frac{e}{e_0}$$

$$- c_w \ell n \frac{T_c}{T_0} \qquad (E.7)$$

The nonequilibrium vapor pressure term and the non equilibrium temperature term in the above equations may be separated as follows,

$$R_v \ell n \frac{e}{e_0} = R_v \ell n \frac{e}{e_{sat}(T)} + R_v \ell n \frac{e_{sat}(T)}{e_0}$$

$$c_w \ell n \frac{T_c}{T_0} = c_w \ell n \frac{T_c}{T} + c_w \ell n \frac{T}{T_0}$$

Using these results in (E.7), the result is

$$s_v(T) - s_c(T) = \left(s_v(T_0) - s_c(T_0)\right) + (c_{pv} - c_w)\ell n \frac{T}{T_0}$$

$$- R_v \ell n \frac{e_{sat}(T)}{e_0} - c_w \ell n \frac{T_c}{T} - R_v \ell n \frac{e}{e_{sat}(T)} \qquad (E.8)$$

Since the reference state is also an equilibrium state, the first term is evaluated as,

$$s_v(T_0) - s_c(T_0) = \frac{\ell_v(T_0)}{T_0} \qquad (E.9)$$

Substituting Equations E.7 and E.9 into Equation E.8, the result is,

$$s_v(T) - s_c(T_c) = \frac{\ell_v(T)}{T} - R_v \ln (RH) - c_w \ln \frac{T_c}{T} \qquad (E.10)$$

where $RH = e/e_{sat}(T)$.

If Equation E.10 is used in the entropy flux equation, (E.6), the resulting equation is written,

$$\begin{aligned} F_S(x) = {} & Q_d s_d(T_0) + Q_w s_c(T_0) - Q_d c_{pd} \ell n\, T_0 + Q_d R_d \ell n\, P_{d_0} \\ & - Q_w c_w \ell n\, T_0 + Q_d (c_{pd} \ell n\, T - R_d \ell n\, P_d) + Q_w c_w \ell n\, T_c \\ & + \rho_v UA \left(\frac{\ell_v(T)}{T} - R_v \ell n\, (RH) \right) - \rho_v UAc_w \ell n \frac{T_c}{T} \end{aligned} \qquad (E.11)$$

The first five terms on the right hand side of (E.11) are constants and they may be combined to give the (conserved) reference state entropy flux, F_{s_0}. Equation E.11 then becomes,

$$\begin{aligned} F_S(x) = {} & F_{S_0} + Q_d \left(c_{pd} \ln T - R_d \ln P_d \right) + \rho_v UA \left(\frac{\ell_v(T)}{T} - R_v \ln (RH) \right) \\ & + \rho_v UAc_w \ln T + \rho_c U_c Ac_w \ln T_c \end{aligned} \qquad (E.12)$$

For the case of no droplets ($\rho_c \to 0$), this entropy flux relation reduces to Equation 2.2.3, which describes the isentropic expansion or contraction of the moist air.

In summary, the entropy equation (E.12) states that, for steady-State assumptions, the entropy flux crossing a cross-sectional area of an adiabatically insulated spray and moist air system is constant. The state of the system is then described for all cross-sections and at all times.

APPENDIX F

FINITE-DIFFERENCES AND NUMERICAL PARAMETERS

Since the systems of equations describing single droplet and droplet ensemble motion in an icing tunnel are closed, the differential equations may be solved numerically. In this study, the equations are programmed in FORTRAN IV language for solution on a digital computer. The derivatives are approximated using an explicit Eulerian finite-difference scheme. Boundary conditions are specified at the plenum (beginning of contraction section) and at the position of the sprayers. For a listing of the programs, the reader is referred to Appendix H.

The explicit Eulerian finite-difference scheme is first order accurate and is the simplest finite-differencing scheme available. Since the differential equations used in this study are complex, it is desirable to use a simple finite-difference scheme. The disadvantage of using the Eulerian scheme is that a small grid spacing must be used in order to reduce the effects of numerical truncation error and to reduce computational instability. The use of a grid spacing smaller than some optimum size, however, is uneconomical. The optimum grid spacing, defined as the maximum grid spacing needed to obtain solutions of given accuracy, is not constant over the tunnel length since it is dependent upon the behaviour of the solutions.

In the present study, the grid spacing is a function of the tunnel geometry. Consequently, any scheme for determining grid spacings is tunnel specific. In most cases, however, the grid spacing near the sprayers has to be very small relative to the spacing at other positions further along the axis since large accelerations of the droplets occur

near the sprayers.

The vertical cross-section of the contraction section of the NRC tunnel consists of a rapidly converging bell-mouth (circular cross-section) followed by a more gentle linear contraction. The cross-sectional area of the bell-mouth contraction for $x \leq 0.1524$ is given by,

$$A = 4\left[0.3810 - (0.02323 - (x - 0.1524)^2)^{\frac{1}{2}}\right]^2$$

The cross-sectional area of the linear contraction is described by,

$$A = 4\left[0.2286 - (0.03846(x - 0.1524)\right]^2$$

For both the single droplet and the ensemble models, optimum grid spacings are determined from the requirement that the uncertainty in the solutions resulting from a choice of the grid spacings is less than the uncertainty in the solutions resulting from errors in the measurement of the tunnel dimensions. The approach adopted is to increase the grid spacings for successive runs using the same initial conditions until the difference between the calculated properties at the working section and some "standard" properties exceeds an acceptable error (i.e. the uncertainty associated with measurement errors). The properiees considered here are the temperature and velocity of the spray and the moist air. The "standard" values of these properties are determined from a run that uses very small grid spacings and is restricted by a very small error limit (to be discussed later). The initial conditions used in calculating these properties are discussed in Section 4.1.

The grid spacing scheme used for the NRC high speed icing tunnel employs logarithmic increments for sections of the tunnel near the sprayers and equispaced increments for sections of the tunnel where the perimeter of a cross-section varies linearly with the x-distance. The details of this incrementation scheme are given in Table F.1.

TABLE F.1

GRID SPACING PARAMETERS USED TO SOLVE FOR FLOW

IN THE NRC HIGH SPEED ICING TUNNEL

X-Range (m)	Increment Type	Number of Increments	Equation for Incremented Position (m)
0.2 - .202	Log	1000	$x_2 = e^{(\ell n x_1 + 10^{-5})}$
.202 - .3	Log	1500	$x_2 = e^{(\ell n x_1 + 10^{-4})}$
.3 - 2.1336	Linear	4000	$x_2 = x_1 + .46 \times 10^{-13}$

The grid spacings shown in Table F.1 are obtained using an assumption that the dimensions of the NRC tunnel can be measured to a tenth of a millimetre. The results of two numerical experiments that vary the tunnel dimensions by amounts of the uncertainty in the measurements are summarized in Table F.2. (The relative changes given in this Table are percentage diviations from the "standard" properties that are obtained for the "actual" tunnel dimensions). In the first experiment, the radius of the bell-mouth contraction is decreased by .0001 m to a value of .1523 m. The second experiment reduces the slope of the linear contraction by an amount of .0001 (units of vertical distance per unit of x-distance) so that the altered cross-sectional area varies more slowly than the actual cross-sectional area.

TABLE F.2

RELATIVE UNCERTAINTIES IN THE SOLUTIONS TO THE ENSEMBLE MODEL RESULTING FROM HYPOTHETICAL MEASUREMENT ERRORS. THESE RESULTS ARE OBTAINED FOR FLOW IN THE NRC HIGH SPEED ICING TUNNEL.

Hypothetical Measurement Error	Percentage variation in solutions at the working section from the standard			
	U (m/s)	U_c (m/s)	T (°K)	T_c (°K)
Slope of linear contraction from .03846 to .03845	1.6×10^{-3}	4.0×10^{-4}	$3.0 \times 10^{-}2$	2.0×10^{-2}
Radius of bell-mouth contraction decreased from .1524M to .1523M	1.2×10^{-1}	3.0×10^{-2}	2.3	2.1

The conclusion from Table F.2 is that a smaller uncertainty (in the final solutions) results from an error in measuring the slope than from an error in measuring the radius. The experiments indicate that the temperatures are more sensitive to changes in these tunnel dimensions than are the velocities. In order to determine the optimum grid spacings with the best precision, the acceptable error for this particular study is chosen as the smallest uncertainty appearing in Table F.2. Hence, the grid spacings of the NRC tunnel that are given in Table 4.1 are obtained from the requirement that the calculated spray velocity at the working section differs from the "standard" value by not more than .0004 percent.

This requirement is more stringent than necessary because of the uncertainty associated with using averaging techniques.

In the single droplet model, the equations for the moist air flow can be integrated to give a velocity equation, (2.2.10). For the ensemble models, on the other hand, the equations describing the coupled air flow are written in finite-difference form and are solved simultaneously by iterative techniques for the moist air variables P, T, and U.

The initial estimate of the velocity needed to solve this system of equations assumes incompressible flow. Letting the subscript 2 denote unsolved variables at the position x_2 and letting the subscript 1 denote solved variables at the position x_1, the following steps are used to solve for the unknown variables in the ensemble model:

1. The droplet properties at position x_2 are obtained from the droplet flow equations (2.4.4, 2.5.1, 2.5.7). These finite-difference equations are written in terms of the known moist air and droplet properties at the position, x_1.
2. These calculated droplet properties are used to determine the mixing ratio of the moist air at position x_2 from the mass conservation relations,

$$Q_d = \rho_d UA = \text{constant} = Q_{d_0}$$

$$Q_w = \rho_w UA + \rho_c U_c A = \text{constant} = Q_{w_0}$$

Since $\rho_v UA = r Q_{d_0}$, the mixing ratio may be obtained using the expression,

$$r = \frac{Q_{w_0} - Q_w}{Q_{d_0}}$$

3. An initial estimate of the moist air velocity, U_2, is calculated from the assumption that the air flow is incompressible.
4. Using the estimated velocity U_2, the moist air pressure P_2 at position x_2 is obtained by solving the global momentum equation (3.3.4). The result is the estimated pressure, P_2.
5. The estimated variables, U_2 and P_2, are then substituted into the entropy flux equation (3.2.1) in order to solve for the variable, T_2.
6. An improved estimate of the velocity U_2, is obtained by substituting P_2 and T_2 into a relation obtained by combining the continuity equation for the dry air and the equation of state. The relation is,

$$U = \frac{Q_{d_0} R_d T'(1+r)}{P_2 A_2}$$

7. If the absolute value of the relative difference between the improved estimate of the velocity and the preceding estimate is greater than an acceptable relative error, EPS2, steps 4 to 6 are repeated until the relative difference is less than EPS2.

For both of the computer models, it is necessary to determine a value for the acceptable error limit that terminates the iterations needed to solve for the air velocity. In the case of the single droplet model, the iterative equation (2.2.10) is considered to be solved when successive improved velocity estimates differ by amounts less than EPS2. When the equations for the air and spray motions are coupled (i.e. the ensemble model), it is seen in step 7 above that the parameter EPS2 plays a similar role.

The procedure used in determining EPS2 is similar to that used in determining the grid spacings. The value of EPS2 is increased for

successive runs until the last increase produces calculated properties at the working section that differ from the "standard" properties by amounts exceeding the uncertainty of the solutions. Values of EPS2, as well as the range of the absolute errors incurred in iterating for the velocity, are summarized in Table F.3. In this study, the value of EPS2 used is 10^{-9},

TABLE F.3

ACCEPTABLE UNCERTAINTY LIMITS AND THE ACTUAL RESIDUALS THAT RESULT FROM ITERATION FOR THE AIR VELOCITY IN THE NRC HIGH SPEED ICING TUNNEL

Acceptable relative uncertainty in air velocity (EPS2)	Equations solved	Number of iterations (n) to solve for velocity	Range of Magnitudes of the relative errors (E) resulting from iteration $E = \frac{\lvert U_n - U_{n-1} \rvert}{U_n}$
10^{-8}	(2.2.10)	4 - 9	4×10^{-10} - 10^{-8}
10^{-9}	Global Equations	3 - 6	2×10^{-11} - 10^{-9}

A test of the accuracy of the solutions to the finite-difference equations for the moist air flow may be performed by comparing the results obtained from the single droplet model to those obtained from the ensemble model if it is assumed that the initial liquid water content is zero. Since the moist air equations may be integrated analytically for the single droplet model, this comparison provides a reasonably good check on the

behaviour of the solutions to the ensemble model.

For flow in the NRC high speed icing tunnel, calculations from the two models (using identical initial conditions) indicate that the two sets of solutions vary by negligible amounts (less than 10^{-4} percent). The two sets of solutions are compared in Table F.4.

TABLE F.4

A COMPARISON OF RESULTS FROM THE SINGLE DROPLET MODEL TO THOSE FROM THE ENSEMBLE MODEL (LWC = 0) FOR SIMILAR INITIAL CONDITIONS. THESE RESULTS DESCRIBE FLOW IN THE NRC HIGH SPEED ICING TUNNEL

Model	Solutions at working section			
	U (m/s)	U_c (m/s)	T (°K)	T_c (°K)
Ensemble (Numerical Solution)	119.9976	105.5773	268.2351	269.9343
Single Droplet (Analytical Solution)	119.9976	105.5772	268.2349	269.9342
Absolute Difference	0	0.0001	0.0002	0.0001
Percentage Difference	0	9.5×10^{-5}	7.5×10^{-5}	3.7×10^{-5}

APPENDIX G

PHYSICAL CONSTANTS AND RELATIONS

In order to calculate a number of terms in the equations for the heat and kinetic energy transfers, it is necessary to know the values of a number of constants and to compute parameters that are functions of known variables. All temperature dependencies in the following relations are written in terms of a temperature, T, measured in degrees Kelvin.

1. The constants that are given below are found in the Smithsonian Meteorological Tables:

$R_d = 287.05 \text{ J kg}^{-1} \text{ °K}^{-1}$

$R_v = 461.51 \text{ J kg}^{-1} \text{ °K}^{-1}$

$\rho_w = 1000. \text{ kg m}^{-3}$

σ = Stefan-Boltzmann constant $= 5.6687 \times 10^{-8} \text{ J m}^{-2} \text{ s}^{-1} \text{ °K}^{-4}$

$c_{pd} = 1005 \text{ J kg}^{-1} \text{ °K}^{-1}$, $c_{pv} = 1850 \text{ J kg}^{-1} \text{ °K}^{-1}$

$c_{vd} = 718 \text{ J kg}^{-1} \text{ °K}^{-1}$, $c_{vv} = 1390 \text{ J kg}^{-1} \text{ °K}^{-1}$

2. Since the tabulated emissivities of a water droplet are not readily available, the emissivity is approximated using the emissivity of a plane water surface. The emissivity of water, E, displays a weak linear dependence on water temperature. The linear dependence is ignored in this study for the range of droplet temperatures considered and a value of E = 0.96 is used.

The approximation of the emissivity of a droplet by that of a plane water surface is not justified when the wavelength of a radiation compares to a droplet radius.

3. The dynamic viscosity of air as a function of temperature is given by (List, 1966, p. 394)

$$\mu = 1.8325 \times 10^{-5}\left(\frac{296.16 + 120}{T + 120}\right)\left(\frac{T}{296.16}\right)^{3/2}$$

The units of viscosity are in $K_g\ m^{-1}\ s^{-1}$.

4. The diffusivity of water vapor in air for temperatures between -40°C and 40°C is given by (Pruppacher and Klett, 1978, p. 413):

$$\mathscr{D} = 0.211 \times 10^{-4}\left(\frac{1013.25}{P}\right)\left(\frac{T}{273.15}\right)^{1.94}$$

The units of diffusivity are $m^2\ s^{-1}$.

5. The specific heat capacity of water as a function of temperature is (Ibid, p. 89)

$$c_w = 4186.84\left[0.9979 + 3.1 \times 10^{-6}(T - 308{,}15)^2 + 3.8 \times 10^{-9}(T - 308.15)^4\right] \qquad \text{for } T \geq 273°K$$

and,

$$c_w = 4186.84\left[1.0074 + 8.29 \times 10^{-5}(T - 273.15)^2\right] \qquad \text{for } T \leq 273°K$$

The units for c_w are $J\ k_g\ °K^{-1}$

6. The saturation vapor pressure as a function of temperature is calculated from the following polynomial in nested form (Lowe, 1977),

$A_0 = 6984.505294$, $A_1 = 188.9039310$

$A_2 = 2.133357675$, $A_3 = -1.2885809730 \times 10^{-2}$

$A_4 = 4.393587233 \times 10^{-5}$ $A_5 = -8.023923082 \times 10^{-8}$

$A_6 = 6.136820929 \times 10^{-11}$

$$e_{sat}(T) = A_0+T(A_1+T(A_2+T(A_3+T(A_4+T(A_5+A_6T)))))$$

e_{sat} is expressed in mb.

7. The surface tension of water in air is (Pruppacher and Klett, 1978, p. 104)

$$\sigma'_{W/A} = 10^{-3}\left[76.10 - .155(T_c - 273.15)\right] \quad \text{for } T \geq 233°K$$

The units of surface tension are J m^{-2}.

8. The specific latent heat of vaporization as a function of temperature is expressed by the following empirical relation (Ibid, p. 89):

$$\ell_v = 4186.84\left[597.3\left[\frac{273.15}{T}\right]^{(.167+3.67\times10^{-4}T)}\right] \qquad \text{(a)}$$

where ℓ_v is expressed in J kg^{-1}.

Alternatively, the specific latent heat of vaporization obtained by integrating Kirchhoff's Law is,

$$\ell_v = 2.501 \times 10^6 - 2340.8(T - 273.15) \qquad \text{(b)}$$

The experimental relation for specific latent heat (Equation a) is used in the droplet thermodynamic and growth equations. Equation b, on the other hand, is used in the entropy flux equation of the ensemble model. The reason for using Equation b rather than Equation a is that the assumptions used in its derivation are then consistent with

some of the assumptions needed to derive the global entropy equation.

9. A relation for the thermal conductivity of moist air is given by Beard and Pruppacher (1971) and by Pruppacher and Klett (1978, p. 418). The author wishes to indicate that the expression given by either reference contains typographical errors.

The thermal conductivity of moist air can be given in terms of the thermal conductivity of dry air, k_d, and of water vapor, k_v. The relation is obtained from the Mason-Saxena formula (see Bird et al, 1960, p. 258) for a gas mixture consisting of dry air and water vapor, where the amount of each gas is expressed in terms of its mole fraction (i.e. the ratio of the partial pressure of the gas to the total pressure). Since the mole fraction of water vapor in moist air is small, the thermal conductivity of moist air may be approximated by a first-order expansion of the Mason-Saxena formula. The result of the approximations is an expression given in terms of k_d and k_v,

$$k = k_d \left[1 - (1.17 - 1.02 k_v/k_d) \frac{r}{r+\varepsilon} \right]$$

The constants in this relation are approximated using data for the viscosity of dry air and of water vapor.

The temperature dependencies of k_d and k_v (Pruppacher and Klett, 1978, p.418) are given by,

$$k_d = 4.1868 \times 10^{-3} \left[5.69 + .017(T - 273.15) \right]$$

$$k_v = 4.1868 \times 10^{-3} \left[3.78 + .020(T - 273.15) \right]$$

The units of conductivity are given in $J\ m^{-1}\ s^{-1}\ {}^{\circ}K^{-1}$.

APPENDIX H

PROGRAM LISTING

```
C ***********************************************************
C ***  THE DROPLET ENSEMBLE PROGRAM CALCULATES THE FLOW
C ***  PROPERTIES OF AN ENSEMBLE OF DROPLETS THAT ARE
C ***  ACCELERATING DUE TO THE AERODYNAMIC DRAG OF AN
C ***  ACCELERATING MOIST AIR FLOW. UNITS USED ARE MKS.
C ***********************************************************
C *** THE VARIABLES USED IN THE PROGRAM ARE GIVEN BELOW.
C *** NOTE THAT VARIABLES ENDING IN SUBSCRIPT 2 REFER TO
C *** CURRENT (UNKNOWN) VALUES. THE SUBSCRIPT 1 IS USED
C *** TO DESCRIBE VALUES OBTAINED FROM THE PREVIOUS
C *** CALCULATION. VARIABLES ENDING IN 0 DENOTE VALUES
C *** THE PLENUM.
C
C ***      VARIABLES
C ***      ---------
C ***      X       AXIAL DISTANCE FROM PLENUM
C ***      AREA     FLOW CROSS-SECTIONAL AREA
C ***      VELX     ONE-DIMENSIONAL VELOCITY OF MOIST AIR
C ***      TD       TEMPERATURE OF MOIST (AND DRY) AIR
C ***      P        PRESSURE OF MOIST AIR
C ***      UC       ONE-DIMENSIONAL VELOCITY OF  DROPLETS
C ***      TC       TEMPERATURE OF DROPLETS
C ***      TVIRT    VIRTUAL TEMPERATURE OF MOIST AIR
C ***      RAD      DROPLET RADIUS
C ***      ROD      DENSITY OF DRY AIR
C ***      RHO      DENSITY OF MOIST AIR
C ***      N        NUMBER OF DROPLETS PER UNIT VOLUME
C ***      ROS      MASS OF WATER DROPLETS PER UNIT VOLUME
C ***      RMIX     MIXING RATIO OF MOIST AIR
C ***      SPH      SPECIFIC HUMIDITY OF MOIST AIR
C ***      RH       RELATIVE HUMIDITY OF MOIST AIR
C ***      FD       MASS FLUX OF DRY AIR
C ***      FA       MASS FLUX OF MOIST AIR
C ***      FV       MASS FLUX OF VAPOR
C ***      FS       MASS FLUX OF SPRAY (DROPLETS)
C ***      FW       MASS FLUX OF WATER SUBSTANCE
C ***      ES       SATURATION VAPOR PRESSURE OF MOIST AIR
C ***      EA       VAPOR PRESSURE OF MOIST AIR
C ***      FNUM     DROPLET NUMBER FLUX
C ***      MASS     DROPLET MASS
C
C *** THE FOLLOWING CONSTANTS, DERIVED PARAMETERS AND
C *** VARIBLES ARE REQUIRED IN THE CALCULATIONS :
C ***
C ***      CONSTANTS
C ***      ---------
C
C ***      SIG     STEFAN-BOLTZMANN CONSTANT
C ***      EMIS    EMISSIVITY OF WATER
C ***      DENS    DENSITY OF WATER
C ***      RD     :GAS CONSTANTS FOR DRY AIR AND
C ***      RV     :WATER VAPOR, RESPECTIVELY
C ***      CPD    :RESPECTIVE SPECIFIC HEAT CAPACITIES AT
C ***      CPV    :CONSTANT PRESSURE
C ***      CVD    :RESPECTIVE SPECIFIC HEAT CAPACITIES AT
C ***      CVV    :CONSTANT VOLUME
```

```
C ***      DERIVED PARAMETERS AND VARIABLES
C ***      ---------------------------------
C
C ***      VIS     VISCOSITY OF AIR
C ***      RE      REYNOLDS NUMBER
C ***      NU      NUSSELT NUMBER
C ***      SH      SHERWOOD NUMBER
C ***      PR      PRANDTL NUMBER
C ***      SC      SCHMIDT NUMBER
C ***      DIFF    DIFFUSIVITY OF MOIST AIR
C ***      TENS    SURFACE TENSION OF WATER IN AIR
C ***      CURV    FACTOR INCREASING THE DROPLET SATURATION
C ***              VAPOR PRESSURE DUE TO CURVATURE EFFECT
C ***      K       THERMAL CONDUCTIVITY OF MOIST AIR
C ***      CP      SPECIFIC HEAT CAPACITY AT CONSTANT
C ***              PRESSURE FOR MOIST AIR
C ***      CV      SPECIFIC HEAT CAPACITY AT CONSTANT
C ***              VOLUME FOR MOIST AIR
C ***      VHEAT   SPECIFIC LATENT HEAT (EMPIRICAL
C ***              RELATION USED IN DROPLET EQUATION)
C ***********************************************************
C ******* CALCULATIONS FOR SPRAY AND AIR FLOW ***************
C ******* PROPERTIES BEGINNING AT THE SPRAYERS.**************
C *** FIRST, CALCULATE  THE MOIST AIR PROPERTIES
C *** AT THE SPRAYERS. THE CALCULATIONS ASSUME FRICTIONLESS
C *** ADIABATIC FLOW (DETERMINED BY INITIAL CONDITIONS
C *** AT THE PLENUM). PART TWO OF THE PROGRAM
C *** CALCULATES THE COUPLED FLOW OF AIR AND SPRAY.
C *** A VARIABLE GRID SPACING IS USED.
C *** X1 IS THE SPRAYER LOCATION. XMAX INDICATES THE
C *** BEGINNING OF THE WORKING SECTION.
C ***********************************************************
      IMPLICIT REAL*8(A-H,O-Z)
      REAL SCALE*8(3),CFIG1(10),CFIG2(10),TITLE(10)
      REAL*8 PI/3.1415926535898/,SIG/5.6687D-08/,
     1       EMIS/0.96D0/,DENS /1000.D0/
      REAL*8 RD/287.05D0/,RV/461.51D0/,CPD/1005.D0/,
     1       CPV/1850.D0/, CVD/718.D0/,CVV/1390.D0/
      REAL*8 X2,AREA2,RMIX2,P2,RHO2,VELX2,TD2,UC2,TC2
      REAL*8 N,MASS,NU,LATENT,K
      READ(5,10) P0,TD0,U0,RH
   10 FORMAT(E12.5,F7.2,F8.3,F7.2)
      READ(5,20) RAD,TC1,X1,UC1,ROS
   20 FORMAT(E10.3,F8.3,F7.4,F8.3,F7.2)
C ***********************************************************
C *** THE INCREMENTATION SCHEME DESCRIBED BELOW
C *** APPLIES FOR THE GEOMETRY OF THE NRC TUNNEL.
C
C ***   XMAX = BEGINNING OF THE CONTRACTION SECTION
C
C ***   THE CONTRACTION DISTANCE IS DIVIDED INTO
C ***   3 SECTIONS. THE  FIRST TWO SECTIONS USE
C ***   LOGARITHMIC INCREMENTS.THE INCREMENTS ARE
C ***   DETERMINED FROM THE RELATION,
C ***     DELTA = (LOG(XTWO) - LOG(XONE))/N
C ***   WHERE XONE, XTWO ARE ENDPOINTS OF THE SECTION
C ***   CONSIDERED AND N IS THE NUMBER OF INCREMENTS
C ***   IN THE SECTION. THE THIRD SECTION USES CONSTANT
C ***   INCREMENTS DETERMINED BY THE RELATION,
C ***     DELTA = (XTWO - XONE)/N
C ***   DEL1, DEL2, DEL3 DENOTE THESE INCREMENTS.
C ***
C ***   XC1, XC2 IN THE PROGRAM CORRESPOND TO XONE,
C ***   XTWO OF THE FIRST AND SECOND SEGMENTS.
C *** XOUT SHIFTS OUTPUT FROM EVERY .05 M. TO .10M.
C ***********************************************************
C *** THE MODEL PARAMETER 'EPS' DENOTES THE ALLOWABLE
C *** RELATIVE ERROR AND 'LIM' DENOTES THE MAXIMUM NUMBER
C *** OF ITERATIONS ALLOWED IN SOLVING FOR VELOCITY.
C ***********************************************************
```

```
C
      READ(5,30) XMAX,N1,N2,N3,LIM,EPS,EPS2
   30 FORMAT(F7.4,3I5,I4,2E8.1)
      READ(5,40) XC1,XC2,XCHG
   40 FORMAT(3F9.6)
      RADOUT=RAD/1.0E-06
C ***************************************************************
C *** PROGRAM PRINTS DESCRIPTION OF TUNNEL. ARRAY
C *** 'TITLE' GIVES TUNNEL IDENTIFICATION. ARRAYS
C *** 'CONFIG1', CONFIG2' DESCRIBE TUNNEL GEOMETRY.
C ***************************************************************
C
      READ(3,50) (TITLE(I),I=1,10)
   50 FORMAT(10A4)
      READ(3,60) (CFIG1(I),I=1,10),(CFIG2(I),I=1,10),
     1(SCALE(I),I=1,3)
   60 FORMAT(10A4/10A4/3(A8/))
      DEL1=(DLOG(XC1/X1))/N1
      DEL2=(DLOG(XC2/XC1))/N2
      DEL3=(XMAX-XC2)/N3
      MASS=4./3.*PI*RAD*RAD*RAD*DENS
      N=1.0D-03*ROS/MASS
      AREA0=CS(0.00D00)
      E=RH*VAPOR(TD0)
      PD=P0-E
      RMIX1=0.62198*E/PD
      SPH=RMIX1/(RMIX1+1.)
      TVIRT=TD0*(1.+SPH*0.6077688)
      CP=CPD*(1.+(CPV/CPD-1.)*SPH)
      CV=CVD*(1.+(CVV/CVD-1.)*SPH)
      GAM=CP/CV
      RO0=P0/(RD*TVIRT)
      FA0=RO0*AREA0*U0
      B1=2.0*GAM*P0/(RO0*(GAM-1.))
      B=B1*(U0*AREA0)**(GAM-1.)
      WRITE(6,70) TITLE,XMAX,CFIG1,CFIG2,TD0,P0,U0,RH
   70 FORMAT('1',T12,'THERMODYNAMIC PROPERTIES OF SPRAYS'/
     1       ' ',T13,'AND AIR FLOW IN AN ICING TUNNEL'/
     2       '-',T9,'TUNNEL DESCRIPTION'/
     3       ' ',T9,'------ -----------'/
     4       '0',T9,'TITLE:'/
     5       ' ',T12,10A4/
     6       ' ',T9,'CONTRACTION LENGTH:'/
     7       ' ',T12,F8.4,'  METERS'/
     8       ' ',T9,'CONFIGURATION:'/
     9       ' ',T12,10A4/' ',T12,10A4/
     *       '0',T9,'TUNNEL OPERATING CONDITIONS AT BELL MOUTH'
     1       /  ' ',T12,'TEMPERATURE:',F8.2,
     2       '  DEG-C'/    ' ',T12,
     3       'PRESSURE:',F9.0,'  PASCALS'/
     4       ' ',T12,'AXIAL VELOCITY:',F9.3,'  M/,SEC'/
     5       ' ',T12,'RELATIVE HUMIDITY',F8.2,'  %')
      AREA1=CS(X1)
      U=AREA0*U0/AREA1
C ***************************************************************
C ***** LOOP TO SOLVE FOR MOIST AIR VELOCITY  *************
C *** IF RELATIVE CHANGE IN VELOCITY ESTIMATE IS
C *** GREATER THAN THE ALLOWABLE ERROR EPS, CONTINUE
C *** ITERATIONS. IF NUMBER IS GREATER THAN LIM, PRINT
C *** ESTIMATE, X2, RESIDUAL, NUMBER OF ITERATIONS
C *** AND TERMINATE THE CALCULATIONS.
C ***************************************************
      DO 80 J=1,LIM
        U1=((U0*U0-U*U+B1)/(B/AREA1**(GAM-1.)))**(1./(1.-
     1  GAM))
        ERR1=DABS((U1-U)/U1)
        FN=U1*U1+B*(AREA1*U1)**(1.-GAM)-U0*U0-B1
        KLIM=J
        IF (ERR1.LE.EPS) GO TO 90
        U=U1
   80 CONTINUE
```

```
C
      GO TO 340
C ***************************************************************
C *** SOLVE FOR REMAINING AIR AND DROPLET
C *** PROPERTIES AT SPRAYERS.
C ***************************************************************
   90 CONTINUE
      VELX1=U1
      RHO1=FA0/(AREA1*VELX1)
      ROD=RHO1/(RMIX1+1.)
      P1=P0*(RHO1/RO0)**GAM
      TVIRT=P1/(RD*RHO1)
      TD1=TVIRT/(1.+0.6077688*SPH)
      VIS=1.8325D-05*(296.16+120.)/(TD1+120.)*(TD1/296.16)**
     11.5
C ***************************************************************
C *** IF INJECTION VELOCITY IS CODED -1.0, DROPLETS
C *** MOVE WITH THE AIR VELOCITY. IF INJECTED
C *** TEMPERATURE IS CODED 0.0, DROPLETS ARE INJECTED
C *** WITH AIR TEMPERATURE.
C ***************************************************************
      IF(UC1.EQ.-1.0) UC1=VELX1
      IF(TC1.EQ.0.00) TC1=TD1
C ***************************************************************
C *** CALCULATE DRAG COEFFICIENT
C ***************************************************************
      RE=2.*RAD*RHO1*(VELX1-UC1)/VIS
      ALPH=0.189D00
      BETA=0.632D00
      IF(RE.LT.20) GO TO 100
      GO TO 120
  100 CONTINUE
      IF(RE.GT.1.5) GO TO 110
      ALPH=0.102D00
      BETA=0.955D00
      GO TO 120
  110 CONTINUE
      ALPH=0.115D00
      BETA=0.802D00
  120 CONTINUE
      C1=DENS*CW(TC1)*RAD*RAD/3.D00
      DRAGF=1.+ALPH*RE**BETA
C ***************************************************************
C *** ACCOUNT FOR VENTILATION EFFECTS
C ***************************************************************
      TEMPF=(TD1+TC1)/2.
      DIFF=0.211D-04*(101325./P1)*(TEMPF/273.15)**1.94
      PR=CP*VIS/COND(TD1,RMIX1)
      SC=VIS/(RHO1*DIFF)
      PR1=PR**(1./3.)
      SC1=SC**(1./3.)
      RESRT=DSQRT(RE)
      XVAR=SC1*RESRT
      YVAR=PR1*RESRT
      IF(XVAR.GE.1.4) SH=2.*(0.78+0.308*XVAR)
      IF(XVAR.LT.1.4) SH=2.*(1.00+0.108*XVAR*XVAR)
      IF(YVAR.GE.1.4) NU=2.*(0.78+0.308*YVAR)
      IF(YVAR.LT.1.4) NU=2.*(1.00+0.108*YVAR*YVAR)
      EA=P1*RMIX1/(0.62198+RMIX1)
      TENS=1.0D-03*(76.10-0.155*(TC1-273.15))
      CURV=DEXP(2.*TENS/(DENS*RV*TC1*RAD))
      ES=CURV*100.*VAPOR(TC1)
      EF=(ES+EA)/2.D00
      VHEAT=LATENT(TC1)
      F1=VHEAT*DIFF*SH*(ES-EA)/(2.*RV*TEMPF*
     1(1.-EF/P1))
      K=COND(TD1,RMIX1)
      F2=K*NU*(TC1-TD1)/2.D00
      TRAD=TC1*TC1*TC1*TC1-TD1*TD1*TD1*TD1
      F3=SIG*EMIS*RAD*TRAD
```

```
      FF1=2.*PI*RAD*DIFF*(ES-EA)*SH*VHEAT/(RV*TEMPF*(1.-EF/
     1P1))
      FF2=2.*PI*RAD*K*NU*(TC1-TD1)
      FF3=4.*PI*(RAD*RAD)*SIG*EMIS*TRAD
      DQ=F1+F2+F3
      DTD=DQ/C1
C ***************************************************************
C *** CALCULATE TERMS OF THE GLOBAL ENTROPY EQUATION AT
C *** THE SPRAYER POSITION. ENTROPY TERMS ARE EHUM, EPRESS,
C *** ETC. NOTE THAT THE SPECIFIC LATENT HEAT IS
C *** CALCULATED FROM KIRCHHOFF'S LAW.
C ***************************************************************
      ROS=1.0D-03*ROS
      FS=ROS*UC1*AREA1
      RH=EA/(100.*VAPOR(TD1))
      RHPER=RH*100.
      FS0=ROS*AREA1*UC1
      FD0=ROD*AREA1*VELX1
      FV=RMIX1*FD0
      FW0=FS0+FV
      FNUM0=N*UC1*AREA1
      CPW=4218.D00
      COEFF=FV*CPW+FD0*CPD
      IF(RH.GT.1.0D-03) GO TO 130
      EHUM=0.00D0
      GO TO 140
  130 CONTINUE
      EHUM=FV*RV*DLOG(RH)
  140 CONTINUE
      EPRESS=FD0*RD*DLOG(P1/(RMIX1/0.62198+1.))
      ELAT=FV*SPLAT(TD1)/TD1
      ESENSC=FS*CPW*DLOG(TC1)
      ETEMP=COEFF*DLOG(TD1)
      WRITE(6,150) ROS,RADOUT,TC1,TD1,UC1,VELX1,RHPER
  150 FORMAT('0',T9,'SPRAY PROPERTIES AT NOZZLES:'/
     1       ' ',T12,'LIQUID WATER CONTENT:',F6.2,
     2       '  KGM/CU.M.'/  ' ',T12,'MEAN DROPLET SIZE:'
     3       ,F6.0,'  MICRONS'/ ' ',T12,'SPRAY TEMPERATURE:'
     4       ,F8.2,'  DEG-C'/ ' ',T12,'AIR TEMPERATURE:'
     5       ,F8.2,'  DEG-C'/ ' ',T12,'SPRAY VELOCITY:'
     6       ,F9.3,'  M/,SEC'/  ' ',T12,'AIR VELOCITY:'
     7       ,F9.3,'  M/,SEC'/ ' ',T12,
     8       'RELATIVE HUMIDITY:',F8.2,'  %')
C
      WRITE(6,160) X1,N1,SCALE(1),DEL1,XC1,N2,SCALE(2),DEL2,
     1XC2,N3,SCALE(3),DEL3,XMAX
  160 FORMAT('0',T9,'X-RANGE',T22,'NUMBER',T31,'SCALE',T41,
     1       'INCREMENT'/ ' ',T9,F8.6,'-'/' ',T19,'!',T22,
     2       I5,T29,A8,T40,E13.7/, ' ',T9,F8.6,
     3       '-'/
     4       ' ',T19,'!',T22,I5,T29,A8,T40,E13.7/,
     5       ' ',T9,F8.6,'-'/
     6       ' ',T19,'!',T22,I5,T29,A8,T40,E13.7/,
     7       ' ',T9,F8.6)
      WRITE(6,170)
  170 FORMAT('0',T4,'X',T9,'AIR SPEED',T21,'DROP SPEED',T31,
     1       'AIR TEMP', T41,'DROP TEMP',T53,'PRESS',T61,
     2       'DENSITY',T70,'AREA',T78, 'ERROR',T91,
     3       'ITER'//
     4       ' ',T3,'RH',T11,'RMIX',T23,'LWC',T36,'RADIUS',
     5      T48,  'NUMBER DENSITY'///)
      WRITE(6,320) X1,VELX1,UC1,TD1,TC1,P1,RHO1,AREA1,ERR1,
     1KLIM,RHPER,RMIX1,ROS,RAD,N
      FENT0=ESENSC+ETEMP-EPRESS+ELAT-EHUM
      TD2=TD1
      XOUT=0.25D0
C ***************************************************************
C *** PART TWO OF PROGRAM CALCULATES PROPERTIES OF
C *** COUPLED AIR AND SPRAY FLOWS.
C ***************************************************************
```

```
      DO 330 ICOUNT=2,16000
        IF(X1.GT.XC2) GO TO 180
        IF(X1.LT.XC2) DEL=DEL2
        IF(X1.LT.XC1) DEL=DEL1
        X2=DEXP(DLOG(X1)+DEL)
        DINCR=X2-X1
        GO TO 190
  180   CONTINUE
        X2=X1+DEL3
        DINCR=X2-X1
        IF(X2.LT.XMAX) GO TO 190
        X2=XMAX
        DINCR=XMAX-X1
        XOUT=X2
  190   CONTINUE
        AREA2=CS(X2)
  200   CONTINUE
C ***************************************************************
C *** CALCULATE SPRAY PROPERTIES
C ***************************************************************
        Q=(9.*VIS)/(RAD*RAD*DENS)*DRAGF
        UC2=DSQRT(UC1*UC1+Q*DINCR*(VELX1-UC1))
        IF(UC1.LE.1.0E-06) GO TO 210
        RAD=(RAD*RAD-2.*F1*DINCR/(DENS*VHEAT*UC1))**0.5
        TC2=TC1-DTD*DINCR/UC1
        IF(X2.EQ.XMAX) GO TO 310
        GO TO 220
  210   CONTINUE
        TC2=TC1
  220   CONTINUE
        MASS=4./3.*PI*RAD*RAD*RAD*DENS
        N=FNUM0/(AREA2*UC2)
        FNUM=N*UC2*AREA2
        ROS=MASS*N
        CMOM1=FS*UC1
        FS=ROS*AREA2*UC2
        CMOM2=FS*UC2
        CMOM=CMOM1-CMOM2
        U=VELX1*AREA1/AREA2
        RMIX2=(FW0-FS)/FD0
        COEFF=FV*CPW+FD0*CPD
        TENS=1.0D-03*(76.10-0.155*(TC2-273.15))
        CURV=DEXP(2.*TENS/(DENS*RV*TC2*RAD))
        ES=CURV*100.*VAPOR(TC2)
        FV=RMIX2*FD0
        SPH=RMIX2/(RMIX2+1.)
        PCON=RMIX2/0.62198+1.
        TCON=1.+0.6077688*SPH
        AVCS=(AREA1+AREA2)/2.D0
        FORCE=6.*N*PI*VIS*RAD*(VELX1-UC1)*DRAGF*AREA1*DINCR
C ***************************************************************
C *** LOOP TO SOLVE GLOBAL EQUATIONS FOR AIR PROPERTIES
C ***************************************************************
        DO 230 KK=1,LIM
          UHOLD=U
          PTERM=FD0*((VELX1-UHOLD)+(RMIX1*VELX1-RMIX2*UHOLD)
     1    )+CMOM
          P2=P1+(PTERM-FORCE)/AVCS
          EPRESS=FD0*RD*DLOG(P2/PCON)
          ELAT=FV*SPLAT(TD2)/TD2
          ESENSC=FS*CPW*DLOG(TC2)
          FENT=-ESENSC+EPRESS-ELAT+EHUM
          YT2=(FENT+FENT0)/COEFF
          TD2=DEXP(YT2)
          TVIRT=TD2*TCON
          U=FD0*RD*TVIRT*(1.+RMIX2)/(P2*AREA2)
          ERR2=DABS((U-UHOLD)/U)
          KLIM=KK
          IF(ERR2.LE.EPS2) GO TO 240
  230   CONTINUE
C
        GO TO 360
```

```
C ***************************************************************
C *** CALCULATE QUANTITIES CHARACTERIZING DROPLET
C *** FLOW RATES, PARAMETERS, ETC. THAT ARE FUNCTIONS OF
C *** AIR PROPERTIES. THESE RESULTS ARE USED IN THE
C *** DROPLET FINITE-DIFFERENCE EQUATIONS TO SOLVE FOR
C *** UNKNOWN PROPERTIES AT NEXT INCREMENT.
C ***************************************************************
 240   CONTINUE
       VELX2=U
       EA=P2*RMIX2/(0.62198+RMIX2)
       RH=EA/(100.*VAPOR(TD2))
       IF(RH.GT.1.0D-03) GO TO 250
       EHUM=0.00D0
       GO TO 260
 250   CONTINUE
       EHUM=FV*RV*DLOG(RH)
 260   CONTINUE
       VIS=1.8325D-05*(296.16+120.)/(TD2+120.)*(TD2/296.16)
     1 **1.5
       RHO2=FD0*(1.+RMIX2)/(AREA2*VELX2)
       RE=2.*RAD*RHO2*(VELX2-UC2)/VIS
       ALPH=0.1890000D00
       BETA=0.632D00
       IF(RE.LT.20) GO TO 270
       GO TO 290
 270   CONTINUE
       IF(RE.GT.1.5) GO TO 280
       ALPH=0.102D00
       BETA=0.955D00
       GO TO 290
 280   CONTINUE
       ALPH=0.115D00
       BETA=0.802D00
 290   CONTINUE
       C1=DENS*CW(TC2)*RAD*RAD/3.D00
       DRAGF=1.+ALPH*RE**BETA
 300   CONTINUE
       PR=CP*VIS/COND(TD2,RMIX2)
       TEMPF=(TD2+TC2)/2.
       DIFF=0.211D-04*(101325./P2)*(TEMPF/273.15)**1.94
       SC=VIS/(RHO2*DIFF)
       PR1=PR**(1./3.)
       SC1=SC**(1./3.)
       RESRT=DSQRT(RE)
       XVAR=SC1*RESRT
       YVAR=PR1*RESRT
       IF(XVAR.GE.1.4) SH=2.*(0.78+0.308*XVAR)
       IF(XVAR.LT.1.4) SH=2.*(1.00+0.108*XVAR*XVAR)
       IF(YVAR.GE.1.4) NU=2.*(0.78+0.308*YVAR)
       IF(YVAR.LT.1.4) NU=2.*(1.00+0.108*YVAR*YVAR)
       EF=(ES+EA)/2.D00
       VHEAT=LATENT(TC2)
       F1=VHEAT*DIFF*SH*(ES-EA)/(2.*RV*TEMPF*
     1 (1.-EF/P2))
       K=COND(TD2,RMIX2)
       F2=K*NU*(TC2-TD2)/2.D00
       TRAD=TC2*TC2*TC2*TC2-TD2*TD2*TD2*TD2
       F3=SIG*EMIS*RAD*TRAD
       DQ=F1+F2+F3
       DTD=DQ/C1
       TD1=TD2
       TC1=TC2
       RMIX1=RMIX2
       UC1=UC2
       VELX1=VELX2
       X1=X2
       P1=P2
       RHO1=RHO2
       AREA1=AREA2
```

```
      IF(X2.LT.XOUT) GO TO 330
      XOUT=XOUT+0.05
      IF (XOUT.GT.XCHG) XOUT=XOUT+0.05
  310 CONTINUE
      FF1=2.*PI*RAD*DIFF*(ES-EA)*SH*VHEAT/(RV*TEMPF*(1.-
     1 EF/P2))
      FF2=2.*PI*RAD*K*NU*(TC1-TD1)
      FF3=4.*PI*(RAD*RAD)*SIG*EMIS*TRAD
      RHPER=RH*100.
      WRITE(6,320) X2,VELX2,UC2,TD2,TC2,P2,RHO2,AREA2,
     1 ERR2,KLIM,RHPER,RMIX2,ROS,RAD,N
  320 FORMAT('0',F6.4,4F10.4,F9.0,2F8.4,E13.4,I6/
     1       ' ',F5.1,E13.4,F11.6,2E13.5)
      IF(X2.EQ.XMAX) STOP
  330 CONTINUE
C
      STOP
C ***************************************************************
C *** PRINTOUT IS GIVEN WHEN ITERATIONS REQUIRED TO
C *** SOLVE VELOCITY EQUATION ARE GREATER THAN LIM.
C ***************************************************************
  340 CONTINUE
      WRITE(6,350) U1,X2,FN,J
  350 FORMAT ('-',T5,'U= ', F8.4,' DOES NOT YIELD ROOT OF EQUATION'
     1       /    ' ',T5,'X= ',F10.6,T17,'FUNCTION= ',E10.2,
     2       T40,'NO. OF ITERATIONS  =',I4)
      STOP
C ***************************************************************
C *** PRINTOUT IS GIVEN WHEN ITERATIONS REQUIRED TO SOLVE
C *** GLOBAL EQUATIONS ARE GREATER THAN LIM.
C ***************************************************************
  360 CONTINUE
      WRITE(6,370) VELX2,X2,KLIM
  370 FORMAT('-',T5,'U =',F12.7,'DOES NOT SOLVE SYSTEM'/' ',
     1       T5,'X =',F10.6,T23,'NO. OF ITERATIONS ='
     2       ,I4)
      STOP
      END
C ***************************************************************
C *** SUBPROGRAM TO CALCULATE TUNNEL CROSS-SECTIONAL AREA.
C ***************************************************************
      REAL FUNCTION CS*8(X)
      REAL*8 X,XHOLD1,XHOLD2
      XHOLD1=X-0.1524
      IF(X.GT.0.1524) GO TO 10
      XHOLD2=0.3810-(0.02323-XHOLD1*XHOLD1)**0.5
      CS=4.*XHOLD2*XHOLD2
      RETURN
   10 CONTINUE
      XHOLD2=0.2286-(0.03846*XHOLD1)
      CS=4.*XHOLD2*XHOLD2
      RETURN
      END
C ***************************************************************
C *** SUBPROGRAM TO CALCULATE  SATURATED VAPOR PRESSURE.
C ***************************************************************
      REAL FUNCTION VAPOR*8(T)
      REAL*8 A0,A1,A2,A3,A4,A5,A6,T
      A0=6984.505294
      A1=-188.9039310
      A2=2.133357675
      A3=-1.2885809730D-02
      A4=4.393587233D-05
      A5=-8.023923082D-08
      A6=6.136820929D-11
      VAPOR=A0+T*(A1+T*(A2+T*(A3+T*(A4+T*(A5+A6*T)))))
      RETURN
      END
```

```
C ***************************************************************
C *** SUBPROGRAM TO CALCULATE LATENT HEAT OF EVAPORATION
C *** USING AN EMPIRICAL RELATION. RESULT IS USED IN
C *** CALCULATIONS FOR DROPLET EQUATIONS.
C ***************************************************************
      REAL FUNCTION LATENT*8(T)
      REAL*8 T
      EXP=0.167+3.67D-04*T
      LATENT=597.3*(273.15/T)**EXP
      LATENT=LATENT*4186.84
      RETURN
      END
C ***************************************************************
C *** SUBPROGRAM TO CALCULATE LATENT HEAT OF EVAPORATION.
C *** RELATION IS DERIVED FROM KIRCHHOFF'S LAW AND IS
C *** USED IN ENTROPY EQUATION.
C ***************************************************************
      REAL FUNCTION SPLAT*8(T)
      REAL*8 T
      SPLAT=-2340.80D00*(T-273.15)+2.501D06
      RETURN
      END
C ***************************************************************
C *** SUBPROGRAM TO CALCULATE SPECIFIC HEAT CAPACITY
C *** OF WATER.
C ***************************************************************
      REAL FUNCTION CW*8(T)
      REAL*8 T,T1
      IF(T.LE.273.15) GO TO 10
      T1=T-308.15
      CW=0.9979+3.1D-06*T1*T1+3.8D-09*T1*T1*T1*T1
      CW=CW*4186.84
      RETURN
   10 CONTINUE
      CW=1.0074+8.29D-05*(T-273.15)*(T-273.15)
      CW=CW*4186.84
      RETURN
      END
C ***************************************************************
C *** SUBPROGRAM TO CALCULATE THERMAL CONDUCTIVITY
C *** OF MOIST AIR.
C ***************************************************************
      REAL FUNCTION COND*8(T,RMIX)
      REAL*8 T,RMIX,EFAC
      DCOND=4.186D-03*(5.69+0.017*(T-273.15))
      VCOND=4.186D-03*(3.78+0.020*(T-273.15))
      EFAC=RMIX/(0.62198+RMIX)
      COND=DCOND*(1.-(1.17-(1.02*VCOND/DCOND))*EFAC)
      RETURN
      END
```